AALTO UNIVERSITY
SCHOOL OF SCIENCE AND TECHNOLOGY
Faculty of Electronics, Communications and Automation

On Optimum Sensing Time over Fading Channels of Cognitive Radio System

Eunah Cho

Master's thesis submitted in partial fulfillment of the requirements for the Degree of Master of Science in Technology

Espoo, Finland, October 2010

Supervisor: Professor Olav Tirkkonen

Instructor: M.Sc. Lu Wei

AALTO UNIVERSITY SCHOOL OF SCIENCE AND TECHNOLOGY

Abstract of the Master's Thesis

Author: Eunah Cho

Title: On optimum sensing time over fading channels for Cognitive Radio system

Date: 29.Oct. 2010 **Number of pages:** 64

Faculty: Electronics, Communications and Automation
Professorship: S-72 Communications Engineering

Supervisor: Professor Olav Tirkkonen
Instructor: M.Sc. Lu Wei

Abstract

Cognitive Radio (CR) is widely expected to be the next Big Bang in wireless communications. In a CR network, the secondary users are allowed to utilize the frequency bands of primary users when these bands are not currently being used. For this, the secondary user should be able to detect the presence of the primary user. Therefore, spectrum sensing is of significant importance in CR networks.

In this thesis, we consider the antenna selection problem over fading channels to optimize the tradeoff between probability of detection and power efficiency of CR systems. We formulate a target function consists of detection probability and power efficiency mathematically, and use energy detection sensing scheme to prove that the formulated problem indeed has one optimal sensing time which yields the highest target function value.

Two modeling techniques are used to model the Rayleigh fading channels; one without correlations and one with correlations on temporal and frequency domains. For each model, we provide two scenarios for average SNRs of each channel. In the first scenario, the channels have distinguished level of average SNRs. The second scenario provides a condition in which the channels have similar average SNRs. The antenna selection criterion is based on the received signal strength; each simulation is compared with the worst case simulation, where the antennas are selected randomly.

Numerical results have shown that the proposed antenna selection criterion enhanced the detection probability as well as it shortened the optimal sensing time. The target function achieved the higher value while maintaining 0.9 detection probability compared to the worst case simulation. The optimal sensing time is varied by other parameters, such as weighting factor of the target function.

Keywords: Cognitive radio; spectrum sensing; energy detector; energy efficiency

Language: English

Acknowledgements

This thesis is based on the work that was carried out in the Communications Laboratory, TKK, from September 2009 to October 2010.

First, my primary thanks for support and priceless knowledge go to the unequaled and eminent professor Olav Tirkkonen. His wide knowledge and his logical way of thinking have been of great value for me. His understanding, encouraging, and personal guidance have provided a good basis for the present thesis.

I also wish to express my warm thanks to M. Sc. Lu Wei for his valuable advice and friendly help. His extensive discussions around my work are interesting explorations have been very helpful for this study.

I would like to thank my friends in Finland and in Korea, for all their support and genuine friendship.

Finally, and most importantly, I wish to thank my family, for their love, support, and encouragement during my whole life.

Espoo, Oct 2010

Eunah Cho

Contents

List of Figures 6

List of Tables 9

List of Abbreviations 10

1 Introduction 10

2 Spectrum Sensing Preliminaries. 13

2.1 Scenario Description. 13

2.2 General Model for Spectrum Sensing. 14

2.2.1 Theory of Hypothesis Testing. 14

2.3 Energy Detector. 16

2.3.1 Test Statistics. 17

2.3.2 Probabilities of Detection and False Alarm. 18

2.3.2.1 Approximations for the Probability of Detection and False Alarm. 21

2.4 Detection over Rayleigh Fading Channels. 21

2.4.1 Fading Channel Modeling. 23

2.4.1.1 Simple Rayleigh Channel Modeling. 24

2.4.1.2 Autoregressive Model. 24

3 Proposed Antenna Selection Methods. 27

3.1 Problem Formulation. 27

3.1.1 From the View of Probability of Detection. 28

3.1.2 From the View of Power Efficiency. 29

3.2 Proposed Scheme. 30

3.2.1 Efficiency of Resources. 31
3.3 Optimum Sensing Time. 33
3.4 Antenna Selection. 34
3.4.1 An Antenna with the Highest Signal Strength. 35
3.4.2 Random Antenna Selection. 35
4 Numerical Results and Discussions. 35
4.1 Non-Fading Channel. 35
4.1.1 Effects of Weighting Factor α. 35
4.1.1.1 Meaningful Range of α. 37
4.1.2 Effects of Sensing Time. 38
4.1.3 Effects of the Number of Antennas. 39
4.1.4 Effects of False Alarm Probability. 40
4.2 Fading Channel. 42
4.2.1 Channels with No Correlations Assumed. 43
4.2.1.1 Channels with Distinguished Average SNR 43
4.2.1.2 Channels with Similar Average SNR 46
4.2.2 Channels with Correlations: AR Modeling. 49
4.2.2.1 Channels with Distinguished Average SNR 49
4.2.2.2 Channels with Similar Average SNR 54
5 Conclusions and Future Work. 58
5.1 Conclusions. 58
5.2 Possible Future Work. 60

List of Figures

Fig. 1 The considered scenario 13
Fig. 2 (a) Theory of hypothesis testing; probability of detection and probability of missed detection 15
Fig. 2 (b) Theory of hypothesis testing; probability of false alarm..... 15
Fig. 3 Block diagram of an energy detector 17
Fig. 4 Complementary ROC ($Pm\ vs.\ Pf$)under rayleigh fading $\bar{\gamma} = 5\ dB, m = 5$. Awgn curve is provided for comparison..... 23
Fig. 5 Probability of detection ($K = 2, N = 400, k = 1$)..... 28
Fig. 6 Example of proposed scheme for k antennas and n samples 30
Fig. 7 Efficiency curve ($K = 8, N = 200$)..... 32
Fig. 8 Target function over non-fading channels($K = 2, N = 400, P_f = 0.1$) 36
Fig. 9 Target function over non-fading channels for different α values..... 37
Fig. 10 Target function over non-fading channels($K = 2, N = 800, P_f = 0.1$) 38
Fig. 11 Detection probability over non-fading channels ($K = 2, N = 800, Pf = 0.1$) 39
Fig. 12 Efficiency function curve ($K = 2, N = 800, P_f = 0.1$) 39
Fig. 13 Target function over non-fading channels($K = 3, N = 400, P_f = 0.1$) 40
Fig. 14 Target function over non-fading channels($K = 2, N = 400, P_f = 0.2$) 41
Fig. 15 Detection probability over Rayleigh fading channels for the random antenna selection ($\bar{\gamma} = 3\ dB, -17\ dB$)..... 43
Fig. 16 Target function over Rayleigh fading channels for the random antenna selection ($\bar{\gamma} = 3\ dB, -17\ dB$)..... 43

Fig. 17 Detection probability over Rayleigh fading channels for the proposed selection method ($\bar{\gamma} = 3\ dB, -17\ dB$)..... 44
Fig. 18 Target function over Rayleigh fading channels for the proposed selection method ($\bar{\gamma} = 3\ dB, -17\ dB$) 45
Fig. 19 Detection probability over Rayleigh fading channels for the random antenna selection ($\bar{\gamma} = -4\ dB, -7\ dB$) 46
Fig. 20 Target function over Rayleigh fading channels for the random antenna selection ($\bar{\gamma} = -4\ dB, -7\ dB$) 46
Fig. 21 Detection probability over Rayleigh fading channels for the proposed selection method ($\bar{\gamma} = -4\ dB, -7\ dB$) 47
Fig. 22 Target function over Rayleigh fading channels for the proposed selection method ($\bar{\gamma} = -4\ dB, -7\ dB$) 47
Fig. 23 Detection probability over AR(100) modeled Rayleigh fading channels for the random antenna selection ($\bar{\gamma} = 3\ dB, -17\ dB$) 50
Fig. 24 Target function over AR(100) modeled Rayleigh fading channels for the random antenna selection ($\bar{\gamma} = 3\ dB, -17\ dB$) 50
Fig. 25 Detection probability over AR(50) modeled Rayleigh fading channels for the random antenna selection ($\bar{\gamma} = 3dB, -17dB$)..... 51
Fig. 26 Target function over AR(50) modeled Rayleigh fading channels for the random antenna selection ($\bar{\gamma} = 3\ dB, -17\ dB$) 52
Fig. 27 Detection probability over AR(50) modeled Rayleigh fading channels for the antenna selection based on signal strength ($\bar{\gamma} = 3\ dB, -17\ dB$)..... 53
Fig. 28 Target function over AR(50) modeled Rayleigh fading channels for the antenna selection based on signal strength ($\bar{\gamma} = 3\ dB, -17\ dB$)..... 53
Fig. 29 Detection probability over AR(50) modeled Rayleigh fading channels for the random antenna selection ($\bar{\gamma} = -4\ dB, -7\ dB$) 55
Fig. 30 Target function over AR(50) modeled Rayleigh fading channels for the random antenna selection ($\bar{\gamma} = -4\ dB, -7\ dB$) 55
Fig. 31 Detection probability over AR(50) modeled Rayleigh fading channels for the antenna selection based on signal strength ($\bar{\gamma} = -4\ dB, -7\ dB$)..... 56
Fig. 32 Target function over AR(50) modeled Rayleigh fading channels for the antenna selection based on signal strength ($\bar{\gamma} = -4\ dB, -7\ dB$).... 56

List of Tables

Table 1 Comparison of target function over non-fading channels 41
Table 2 Comparison of target function over Rayleigh fading channels ($\bar{\gamma} = 3\ dB, -17\ dB$)..... 45
Table 3 Comparison of target function over Rayleigh fading channels ($\bar{\gamma} = -4\ dB, -7\ dB$) 48
Table 4 Worst case simulation over AR(100) modeled Rayleigh fading channels ($\bar{\gamma} = 3\ dB, -17\ dB$) 51
Table 5 Comparison on target function over AR(50) modeled Rayleigh fading channels ($\bar{\gamma} = 3\ dB, -17\ dB$)..... 54
Table 6 Comparison on target function over AR(50) modeled Rayleigh fading channels ($\bar{\gamma} = -4\ dB, -7\ dB$) 56

List of Abbreviations

ACF	Autocorrelation Function
AR	Autoregressive
AWGN	Additive White Gaussian Noise
CDF	Cumulative Density Function
CR	Cognitive Radio
CSCG	Circularly Symmetric Complex Gaussian
FCC	Federal Communications Commission
IDFT	Inverse Discrete Fourier Transform
i.i.d	Independent and Identically Distributed
NP	Neyman-Pearson
PDF	Probability Density Function
PSD	Power Spectral Density
PSK	Phase Shift Keying
PU	Primary Users
ROC	Receiver Operating Characteristic
SNR	Signal to Noise Radio
SOS	Sum-Of-Sinusoids
SU	Secondary Users

Chapter 1

Introduction

In recent years, the increasing popularity of diverse wireless technologies has generated a huge demand for more bandwidth. As the interest of consumers in wireless services has been greatly developed, the traditional approach to spectrum regulation has caused a crowded spectrum with most frequency bands already assigned to different licensees [1]. The development of new applications and usage of mobile internet access has caused even higher demand for the spectrum.

It is reported that the allocated spectrum experiences low utilization. In fact, recent measurements by Federal Communications Commission (FCC) have shown that 70% of the allocated spectrum in US is not utilized [2]. These factors have been working as a driving force to draw the concept of spectrum reuse.

Cognitive radio (CR) is the core technology behind spectrum reuse. There have been a large amount of academic research as well as application initiatives in this area. The fundamental idea of CR is to automatically sense and make efficient use of any available radio frequency spectrum at a given time [3]. Two main entities are introduced, primary user and secondary users. Primary users are the owners of the licensed spectrum while the secondary users transmit and receive signals over the licensed spectra or portions of it when the primary users are inactive [1]. Namely, the secondary radio periodically monitors the radio spectrum, intelligently detects occupancy in the different frequency bands and then opportunistically communicates over the spectrum holes with minimal interferences to the active primary users [4]. In order to do so, secondary

users are required to frequently perform spectrum sensing so detection the presence of the primary users should be done properly. It is required for secondary users to detect the presence of active primary users with high probability and empty the channel or limit the transmission power.

Identification and detection of primary user signals, thus, are essential tasks for a CR system. This process gets challenging when there exists wide variety of primary users, secondary user interference, variable propagation losses and thermal noise. Under those harsh and noisy environments, speed and accuracy of measurement are the main metrics to determine the suitable spectrum sensing technique for CR [1].

In a heavily shadowed or fading environment, spectrum sensing is hampered by the uncertainty resulting from channel randomness. In such cases, a low received energy may be due to a faded primary signal rather than a white pace. As such, a secondary user has to be more conservative so as not to confuse a deep fade with a white space, thereby resulting in poor spectrum utilization [18].

In this thesis, simple energy detection is chosen as the underlying spectrum sensing scheme. The energy detector is one of the simplest spectrum sensing methods [5]. It works well when the signal to noise ratio (SNR) is high. However, in wireless channels, signals often suffer from shadowing or fading, which may lead to a very low SNR. Under these circumstances, the energy detector might determine that a deeply shadowed or faded channel is unoccupied, causing large interferences to the primary user [6]. Simulation results of [7] suggest that the performance of energy-detector degrades in shadowing/fading environments.

Using fewer antennas is recommended from a complexity standpoint as the efficiency of system resources including the total transmission power grows approximately linearly with the number of users. We should note that under practical circumstances, spectrum sensing is performed with limited resources [6]. Therefore, the efficiency of resource usage is a crucial design parameter. In order to improve the efficiency of spectrum sensing, finding an optimum number of secondary users has been proposed [6].

The main focus of this thesis is to extend these works [4, 6, 20] by finding an optimum sensing time over fading channels. The performance of

spectrum sensing in fading environments is quantified and the effects of the proposed antenna selection method are studied. Particularly, by taking the resource usage efficiency into account, a novel spectrum sensing algorithm has been devised; after initial sensing, antennas with a more deeply faded channel are selected and removed. Spectrum sensing with relatively less-faded antennas are continued during dedicated sensing. There exists an optimal check point which increases overall performances such as power efficiency and probability of detection.

In this thesis, we focus on the optimal check point for spectrum sensing by accounting for power efficiency. Static additive white Gaussian noise (AWGN) channels and Rayleigh fading channels are examined.

This thesis is organized as follows. In Chapter II, the spectrum sensing methodologies are shown after the system model and notations are introduced. The proposed optimum sensing time and antenna selection scheme will be shown in the Chapter III. Chapter IV presents the numerical results of proposed schemes over fading and non-fading circumstances and discussions on them. Finally in Chapter V we conclude the main results of this thesis.

Chapter2

Spectrum Sensing Preliminaries

In this chapter, the general model for spectrum sensing is presented. Then we introduce the energy detection scheme and analyze the relationship between the probability of detection and the probability of false alarm. We also derive the average detection probability over Rayleigh channel.

2.1 Scenario Description

The primary and secondary users are located in the same area. As shown in Fig. 1, spectrum sensing is performed by a secondary sensing node (SU) which is equipped with multiple antennas. Since neither the locations of the primary transmitters (PU) nor the locations of the primary receivers are known, secondary users have to collect spectrum availability information from the entire region [19].

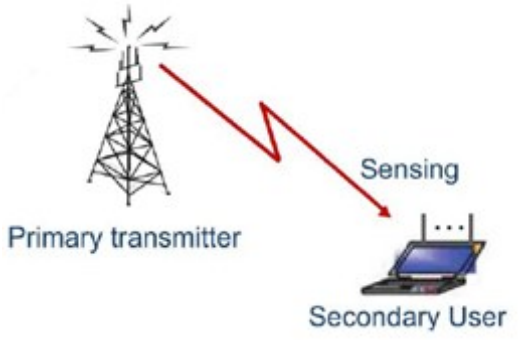

Fig. 1 The considered scenario

2.2 General Model for Spectrum Sensing

The goal of spectrum sensing is to determine if a licensed band is not currently being used by its primary owner. This in turn may be formulated as a binary hypothesis testing problem, which will be discussed in the next part.

We first introduce the signal model that will be employed in our analysis. A Cognitive (or secondary) user detects the presence of ongoing primary user's transmission using a hypothesis test. When the primary user is not active, the received signal at the secondary user can be represented as

$$y(n) = u(n) \tag{1}$$

where y(n) is the signal received by the secondary user and u(n) is noise.

When the primary user is active, the received signal is given by

$$y(n) = h(n)s(n) + u(n) \tag{2}$$

Under this hypothesis, the signal s(n) is transmitted by the primary users and received by secondary users over a channel h(n). When the channel is non-fading, h(n) is constant. On the other hand, when the channel is fading, h(n) includes multipath and fading effects. It is assumed that noise samples u(n) are independently and identically distributed (i.i.d.) with zero mean and variance $E[|u(n)|^2] = \sigma_u^2$. The goal of spectrum sensing is to make a decision, i.e. to choose between H_0 and H_1, based on the received signal [9].

2.2.1 Theory of Hypothesis Testing

We consider a group of N cognitive users in the presence of a primary transmitter. The received signals are corrupted by noise [8]. There are two hypothesis; hypothesis 0, or H_0, denotes the absence of the primary user and hypothesis 1 H_1 denotes the presence of the primary user.

The probability density function (PDF) under each hypothesis is shown in Fig. 2 (a) and in Fig. 2 (b), where the threshold value for each hypothesis is denoted as u. Under each hypothesis the PDFs

are with the difference in means causing the PDF under H_1 to be shifted to the right.

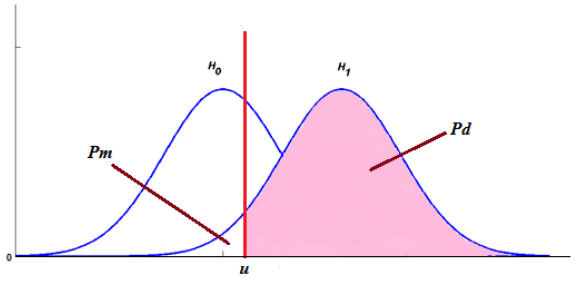

Fig. 2 (a) Theory of hypothesis testing; probability of detection and probability of missed detection

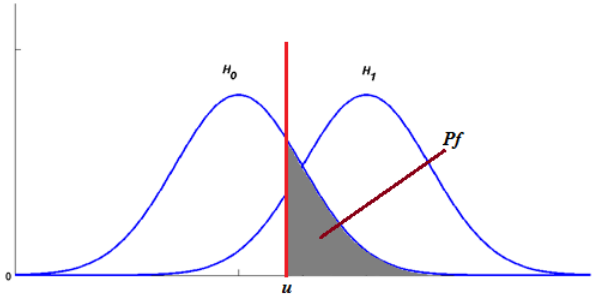

Fig. 2 (b) Theory of hypothesis testing; probability of false alarm

Generally, two probabilities are of interest for indicating the performance of a sensing algorithm.

(i) Probability of detection, P_d, defines the probability of the sensing algorithm having detected the presence of the primary signal at the hypothesis H_1.Thus, in Fig. 2 (a), under the hypothesis H_1, the PDFs bigger than the threshold value u is defined as the detection probability. The PDFs smaller than the threshold u is defined as probability of missed detection, P_m.

(ii) Probability of false alarm, P_f, defines at the hypothesis H_0, the probability of the sensing algorithm claiming the presence of the primary signal. That is, if we decide H_1, but H_0 is true, it is called a false alarm error. In Fig. 2 (b), the PDFs exceeding the threshold under the hypothesis H_0 is defined as P_f.

More methodological approach to these two probabilities will be discussed in the section 2.3.2. This setup is termed the Neyman-Pearson (NP) approach to hypothesis testing or to signal detection. The threshold is found from the false alarm constraint.

Within the context of opportunistic spectrum access, the probability of detection determines the level of interference-protection provided to the primary licensee while the probability of false-alarm is the percentage of white spaces falsely declared occupied. Therefore, a sensible design criterion is to minimize P_f while guaranteeing that P_d remains above a certain threshold set by the regulator.

These two probabilities are unavoidable to some extent but may be traded off against each other. The primary user receives better protection when the probability of detection is high. Also, the secondary user has more chances to find and use the available frequency bands when the probability of false alarm is low.

It is not possible to reduce both error probabilities simultaneously. A typical approach is to hold one probability fixed while minimizing the other [10]. Though there can be different methods to measure the performance of a sensing algorithm, optimization of a sensing algorithm is shown to be achieved when we maximize P_d for a given P_f at a fixed number of samples.

2.3 Energy Detector

The secondary users are required to sense and monitor the radio spectrum environment within their operating range to detect the frequency bands that are not occupied by primary users. In this section we discuss the most popular spectrum sensing scheme, the energy detector.

The energy detector employs a non-coherent detection technique, which does not require prior knowledge of pilot data [1].

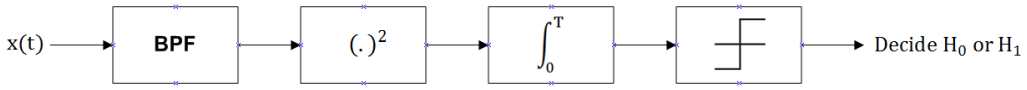

Fig. 3 Block diagram of an energy detector

Fig. 3 depicts the block-diagram of an energy detector. As the figure shows, the energy detector consists of a low pass filter to remove out of band noise and adjacent channel interference, an analog to digital converter as well as a square law device to compute the energy.

The local spectrum sensing is accomplished by the energy detection [7]. An energy detector is implemented at each secondary user by calculating a decision metric out of all samples and antennas used. The purpose of energy detection is to make a correct decision between two hypotheses after observing samples. The energy detection should be carried out over all logical channels defined by the CR network. Assuming that the channel is time-invariant during the sensing process, the energy detection on the given channel is performed by accumulating the energy of samples and comparing it with the predefined threshold, to decide whether signal is present or not [16].

2.3.1 Test Statistics

In order to properly set the stage for the discussion, we start with an analysis of local energy detection. We denote that the normalized output of the integrator in Fig. 3 by T which serves as the decision statistic. The test statistic for the energy detector is given by,

$$T(y) = \frac{1}{N}\sum_{n=1}^{N}|y(n)|^2 \qquad (3)$$

where N is the number of samples. The test statistic T(y) is a random variable whose PDF $p_0(x)$ is a Chi-square distribution with 2N degrees of freedom for complex valued case [11].

2.3.2 Probabilities of Detection and False Alarm

Under hypothesis H_0, if ε is chosen as the detection threshold, the probability of false alarm is then given by

$$P_f(\varepsilon,\tau) = P_r(T(y) > \varepsilon|H_0) = \int_{\varepsilon}^{\infty} p_0(x)dx \tag{4}$$

where τ is the available sensing time.

The PDF of this test statistics under H_0 may be written as,

$$p_0(x) = \frac{x^{m-1}e^{-x/2}}{\Gamma(m)2^m} \tag{5}$$

where m is the time-bandwidth product and $\Gamma(.)$ is the gamma function. After integration, the probability of false alarm is

$$P_f = \frac{\Gamma(m,\varepsilon/2)}{\Gamma(m)} \tag{6}$$

The incomplete gamma function is expressed as

$$\Gamma(a,b) = \int_{b}^{\infty} t^{a-1}e^{-t}dt \tag{7}$$

As expected, P_f is independent of SNR since under H_0 there is no primary signal present.

On the other hand, under the hypothesis H_1, for a chosen threshold ε the probability of detection can be represented as

$$P_d(\varepsilon,\tau) = P_r(T(y) > \varepsilon|H_1) = \int_{\varepsilon}^{\infty} p_1(x)dx \tag{8}$$

where $p_1(x)$ is the PDF of the test static T(y) which can be written as,

$$p_1(x) = \frac{x^{m-1}e^{-\frac{x+2m\gamma}{2}}}{\Gamma(m)2^m} F_I\left(m,\frac{m\gamma x}{2}\right) \tag{9}$$

where $F_I(.,.)$ is the confluent hyper-geometric limit function and γ is the SNR is defined as γ . Therefore, the probability of detection can be written as

$$P_d = Q_m\left(\sqrt{2m\gamma}\,, \sqrt{\varepsilon}\right) \tag{10}$$

The generalized Marcum Q-function $Q_m(.,.)$ is as

$$Q_m(a\,, b) = \int_b^{\infty} \frac{x^m}{a^{m-1}} e^{-\frac{x^2+a^2}{2}} I_{m-1}(ax)dx \tag{11}$$

where $I_{m-1}(.)$ is the $(m-1)$th order modified Bessel function of the first kind.

As discussed above, if the decision is H_0 when there is a primary user present, it is called missed detection and its probability is represented as P_m. The missed detection probability is

$$P_m(\varepsilon) = 1 - P_d(\varepsilon) \tag{12}$$

In the CR system, the probability that the presence of the primary user is not detected should be minimized to prevent unexpected interference to the primary user such that the probability of false alarm is maintained below a certain level. The fundamental tradeoff between P_m and P_f has different implications. High P_m results in missing the presence of primary user with high probability, which in turn increases the interference inflicted on the primary licensee. On the other hand, a high P_f inevitably results in low spectrum utilization since the false-alarms increase the number of missed opportunities.

2.3.2.1 Approximations for the Probability of Detection and False Alarm

In this section, we introduce the approximations for the detection probability and false alarm probability in closed form.

From the central limit theorem, we approximate the probabilities of detection and false alarm as follows. First, for a large N, T(y) can be approximated as a Gaussian random variable with mean

$$\mu = \begin{cases} \sigma_u^2 = \mu_0 & H_0 \\ (\gamma+1)\sigma_u^2 = \mu_1 & H_1 \end{cases} \tag{13}$$

and variance

$$\sigma^2 = \begin{cases} \frac{1}{N}(E|u(n)|^4 - \sigma_u^4) = \sigma_0^2 & H_0 \\ \frac{1}{N}(E|s(n)|^4 + E|u(n)|^4 - (\sigma_s^2 - \sigma_u^2)^2) = \sigma_1^2 & H_1 \end{cases} \quad (14)$$

If we focus on the circularly symmetric complex Gaussian (CSCG) noise case, than the probability of false alarm can be approximated by

$$P_f(\varepsilon, \tau) = Q\left(\left(\frac{\varepsilon}{\sigma_u^2} - 1\right)\sqrt{N}\right) \quad (15)$$

and Q(.) is the complementary distribution function of the standard Gaussian.

$$Q(x) = \frac{1}{\sqrt{2\pi}}\int_x^\infty exp\left(-\frac{t^2}{2}\right)dt \quad (16)$$

We focus on the complex-valued phase-shift keying (PSK) signal and CSCG noise case. Based on the PDF of the test static, the probability of detection can be approximated by

$$P_d(\varepsilon, \tau) = Q\left(\left(\frac{\varepsilon}{\sigma_u^2} - \gamma - 1\right)\sqrt{\frac{N}{2\gamma + 1}}\right) \quad (17)$$

Note that $\gamma = \frac{\sigma_s^2}{\sigma_u^2}$ is the received SNR of the primary user measured at the secondary receiver of interest, under the hypothesis H_1.

The Q function is monotonically decreasing since $1 - Q$ is a cumulative distribution function (CDF), which is monotonically increasing. Thus, Q has an inverse that we denote as Q^{-1}. Therefore, equation (17) can be represented in a different way for the detection threshold ε,

$$\left(\left(\frac{\varepsilon}{\sigma_u^2} - \gamma - 1\right)\sqrt{\frac{N}{2\gamma + 1}}\right) = Q^{-1}(\bar{P}_d) \quad (18)$$

where the target probability of detection is denoted as $\bar{P}_d$. Also, for the probability of false alarm, the equation can be shown as

$$\left(\frac{\varepsilon}{\sigma_u^2}-1\right)\sqrt{N}=Q^{-1}(P_f) \tag{19}$$

Thus, the equation of P_f can be changed into the equation of $Q^{-1}(\bar{P}_d)$. As

$$\underbrace{\left(\frac{\varepsilon}{\sigma_u^2}-\gamma-1\right)\sqrt{\frac{N}{2\gamma+1}}}_{Q^{-1}(\bar{P}_d)}\times\sqrt{2\gamma+1}=\underbrace{\left(\frac{\varepsilon}{\sigma_u^2}-1\right)\sqrt{N}}_{Q^{-1}(P_f)}-\sqrt{N}\gamma \tag{20}$$

$$P_f=Q\left(Q^{-1}(\bar{P}_d)\sqrt{2\gamma+1}+\sqrt{N}\gamma\right) \tag{21}$$

In a similar way, the probability of detection for a target probability of false alarm is given by

$$P_d=Q\left(\frac{1}{\sqrt{2\gamma+1}}\left(Q^{-1}(\bar{P}_f)-\sqrt{N}\gamma\right)\right) \tag{22}$$

2.4 Detection over Rayleigh Fading Channels

In the previous section, we discussed the detection scheme over non-fading channel. The exact expression of detection probability is given in (10) and the probability of false alarm is given in (6).

In a fading environment, unlike non-fading environment, the distributions and consequential probabilities do not follow previously given formulas anymore since the SNR has different distributions. Note that the probability of false alarm, however, remains the same under any fading channel since it is considered for the case of no signal transmission and as such is independent of SNR [7].

On the other hand, when the channel is varying because of fading effects, previously given equations on probability of detection represents probability of detection conditioned on the instantaneous SNR. Therefore, by averaging the conditional probability of detection over the SNR fading distribution, we can find the expressions in closed form of detection probability in fading channels.

$$P_{d,fading} = \int_{\gamma} Q_m\left(\sqrt{2m\gamma}, \sqrt{\varepsilon}\right) f_{\gamma}(x)dx \tag{23}$$

where $f_{\gamma}(x)$ is the probability of distribution function of SNR under fading.

Under Rayleigh fading, the signal amplitude follows a Rayleigh distribution. In this case, the SNR follows an exponential PDF,

$$f(\gamma) = \frac{1}{\bar{\gamma}} exp\left(-\frac{\gamma}{\bar{\gamma}}\right) \tag{24}$$

where $\bar{\gamma}$ is the average SNR.

Therefore, in Rayleigh fading, a closed-form formula for P_d may be obtained as follows.

$$P_{d,Ray} = \frac{\Gamma\left(m-1, \frac{\varepsilon}{2}\right)}{\Gamma(m-1)} + e^{-\frac{\varepsilon}{2(1+m\bar{\gamma})}}\left(1+\frac{1}{m\bar{\gamma}}\right)^{m-1} \times \left[1 - \frac{\Gamma\left(m-1, \frac{\varepsilon m\bar{\gamma}}{2(1+m\bar{\gamma})}\right)}{\Gamma(m-1)}\right] \tag{25}$$

Fig. 4 illustrates the complementary receiver operating characteristic (ROC) curve of AWGN and Rayleigh fading channel. The average SNR value $\bar{\gamma}$ is assumed to be 5 dB, where m is also selected to be 5.

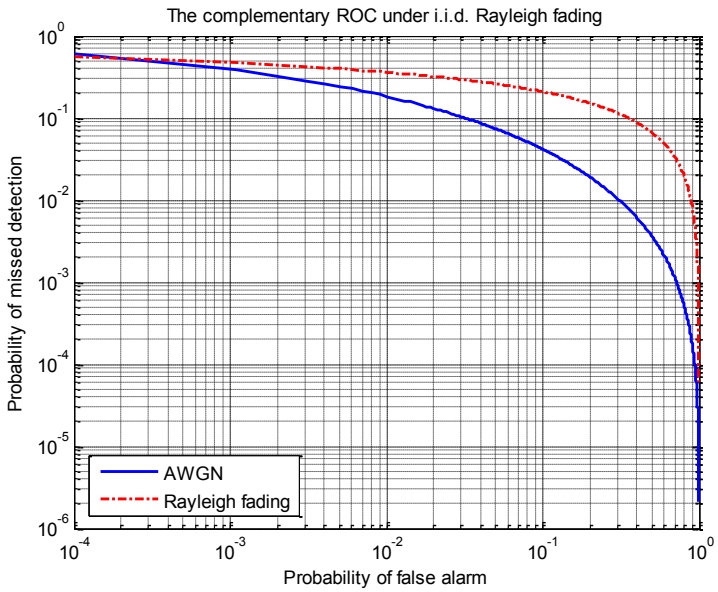

Fig. 4 Complementary ROC (P_m $vs.$ P_f)under Rayleigh fading ($\bar{\gamma} = 5\ dB, m = 5$). AWGN curve is provided for comparison.

We can generally infer that P_m $vs.$ P_f curves have low slopes for $P_f < 0.1$. We also notice that there is a significant effect on the performance of the energy detector by Rayleigh fading. The effect of Rayleigh fading gets more obvious as P_m drops 0.01; P_f reaches up to 0.9, which would result in poor spectrum utilization.

2.4.1 Fading Channel Modeling

The Rayleigh fading process appears in many physical models of mobile radio channels. Many algorithms have been proposed for the generation of correlated Rayleigh variates, such as a sum-of-sinusoids (SOS) approach and the inverse discrete Fourier transform (IDFT) algorithm. Several problems have been found in the designs. For example, in the case of SOS designs, it has been found that the classical Jakes' simulator produces fading signals that are not wide-sense stationary [23]. On the other hand, the IDFT technique has a disadvantage that all samples are generated with a single FFT operation, while it has some advantages on its high quality and the fact that itself works as an efficient fading generator [24]. These motivated the research for a fading simulator which can produce statistically accurate variates [15].

In this thesis, two modeling techniques have been used; one is a simple Rayleigh fading channel assuming a coherent channel, while another one is a general autoregressive (AR) modeling approach for the accurate generation of a time-correlated Rayleigh process.

2.4.1.1 Simple Rayleigh Channel Modelling

Under this modeling, we assume that there is no correlation in temporal and frequency domains. The phase has uniform distribution and the magnitude is Rayleigh distributed. Simply, the signal can be represented by

$$R = \sqrt{X^2 + Y^2} \tag{26}$$

where $X \sim N(0, \sigma^2)$ and $Y \sim N(0, \sigma^2)$ are two independent normal distributions.

2.4.1.2 Autoregressive Model

A complex AR process of order p can be generated via the time domain recursion

$$x[n] = -\sum_{k=1}^{p} a_k \, x[n-k] + u(n) \tag{27}$$

where u(n) is a complex white Gaussian noise process with uncorrelated real and imaginary components. This process is termed an autoregression in that the sequence x[n] is a linear regression on itself with u(n) representing the error [13]. For generating Rayleigh variates the driving noise process u(n) has zero mean and variance σ_u^2. There is a condition on the AR coefficients; all roots of the following polynomial are within the unit disc in the complex plane.

$$\varphi_a(z) = 1 - \sum_{j=1}^{p} a_j z^j \tag{28}$$

Since the frequency response is

$$H(f) = \frac{1}{1 + \sum_{k=1}^{p} a_k exp(-j2\pi fk)} \tag{29}$$

The corresponding power spectral density (PSD) of the $AR(p)$ process is [13]

$$S_{xx}(f) = \frac{\sigma_u^2}{\left|1 + \sum_{k=1}^{p} a_k exp(-j2\pi fk)\right|^2} \tag{30}$$

The relationship between parameters of an AR process and the autocorrelation function (ACF) $r_{xx}[k]$ is [13],

$$r_{xx}[k] = \begin{cases} -\sum_{l=1}^{p} a[l] r_{xx}[k-l] & k \geq l \\ -\sum_{l=1}^{p} a[l] r_{xx}[-l] + \sigma_u^2 & k = 0 \end{cases} \tag{31}$$

These equations are called the Yule-Walker equations. Though there is a nonlinear relationship between the ACF and the parameters of an AR process, when the desired ACF samples $r_{xx}[k]$ for $k = 0, 1, \cdots, p$ are given, we may find the AR model coefficients by solving the set of linear p Yule-Walker equations. In matrix form the upper equations become for $k = 1, 2, \cdots, p$

$$\underbrace{\begin{bmatrix} r_{xx}[0] & r_{xx}[-1] & \cdots & r_{xx}[-(p-1)] \\ r_{xx}[1] & r_{xx}[0] & \cdots & r_{xx}[-(p-2)] \\ \vdots & \vdots & \ddots & \vdots \\ r_{xx}[p-1] & r_{xx}[p-2] & \cdots & r_{xx}[0] \end{bmatrix}}_{R_{xx}} \begin{bmatrix} a[1] \\ a[2] \\ \vdots \\ a[p] \end{bmatrix} = -\begin{bmatrix} r_{xx}[1] \\ r_{xx}[2] \\ \vdots \\ r_{xx}[p] \end{bmatrix} \tag{32}$$

Since $R_{xx}^H = R_{xx}$ and each element along diagonal is the same, R_{xx} is *hermitian Toeplitz*. By using the Levinson-Durbin recursion in $O(p^2)$, these equations may be solved. The matrix R_{xx} inherits the positive semi-definite property from the ACF and it will be singular only if the process is purely harmonic and consists of p-1 or fewer sinusoids [14]. In all other cases, the inverse R_{xx}^{-1} exists and the Yule-Walker equations are guaranteed to have the unique solution

$$a = -R_{xx}^{-1} v \tag{33}$$

where $a = [a[1], a[2], \cdots, a[p]]^p$ and $v = [r_{xx}[1], r_{xx}[2], \cdots, r_{xx}[p]]^T$ [8].

Though AR models have been used with success to predict fading channel dynamics for the purposes of Kalman filter based channel estimation and for long-range channel forecasting, low-order AR processes do not provide a good match to the desired band limited correlation statistics [15].

Chapter 3

Proposed Antenna Selection Methods

In the previous chapter, the relationship between the probability of detection and the probability of false alarm has been established. In this chapter, we study the fundamental tradeoff between probability of detection and power efficiency and discuss how the sensing time can be optimized in order to maximize the probability of detection and the power efficiency.

3.1 Problem Formulation

In this section, we present the detailed formulation of finding the optimal sensing time. First, we start with showing the given conditions. Consider a CR network with K antennas. Each antenna collects N samples during the sensing time. The received $K \times N$ data matrix Y is represented as

$$Y = \begin{pmatrix} y_{1,1} & y_{1,2} & \cdots & y_{1,N} \\ y_{2,1} & y_{2,2} & \cdots & y_{2,N} \\ \vdots & \vdots & \ddots & \vdots \\ y_{K,1} & y_{K,2} & \cdots & y_{K,N} \end{pmatrix} \tag{34}$$

Among several evaluation methods for CR network throughput, we analyze two points of views; one is probability of detection and another is power efficiency.

3.1.1 From the View of Probability of Detection

As mentioned before, when we collect more data from a bigger number of samples N, it is more likely to detect a signal with higher probability. This can be verified by the equation (17) in the previous section.

The probability of detection over the number of samples under a non-fading channel is illustrated in Fig. 5 where the detection probability keeps increasing as more numbers of samples are utilized. In Fig. 5, we have chosen $\mathrm{K} = 2, \mathrm{N} = 400,\ \mathrm{SNR} = -10$ dB and probability of false alarm $\mathrm{P_f} = 0.1$.

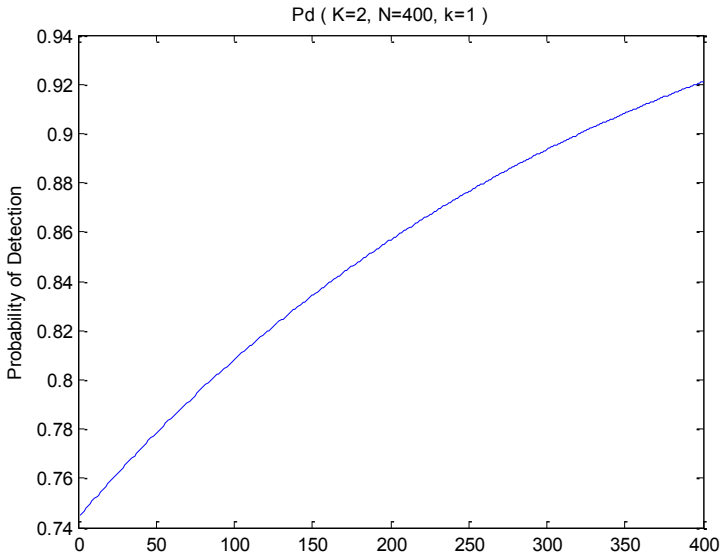

Fig. 5 Probability of Detection ($K = 2, N = 400, k = 1$)

We observe that detection probability increases as more samples are used.

3.1.2 From the View of Power Efficiency

On the other hand, the disadvantage of increasing the number of antennas is a substantial penalty in power consumption due to the required replication of the transmit/receive chains [25]. Also, since sensor networks are typically power limited, we need to invent power allocation strategies that optimally make use of the available radio resources.

Generally speaking, the more samples we collect for the sensing, the more power would be consumed but the higher detection probability would be obtained during the spectrum sensing process. Thus, there exists a tradeoff between power consumption and probability of detection on spectrum sensing; one gets higher probability of detection but has to consume more energy instead. As the sender and the receiver are supposed to spend energy to transmit and receive signals during sensing, intuitively, the power consumed would get lower if we could decrease the number of antennas in use.

Subsequently, one may face the issues regarding selection of antennas; how to select them, what antennas to choose, and by which criteria we choose them. Selecting the antennas which would yield performances would be favorable to achieve improved throughputs, such as probability of detection. With this reason, there have been continuous research efforts on the selection of antennas and sensors in CR networks [6] [16] [20]. Especially under the fading channels, where signals are deteriorated, selection of proper antennas carries more significance.

In the previous section, Fig. 4, we have illustrated that P_f under the Rayleigh fading channel reaches 1 much more drastically comparing to P_f under the AWGN channel. We observed that comparing that of AWGN channel scenario, the detection performance showed significant degradation under Rayleigh fading scenario. Degradation of detection probability endangers detection performance under the hypothesis 1. Therefore, under fading conditions, it becomes even more important to select antennas with less-faded channels to maintain a certain level of performance.

3.2 Proposed Scheme

Above, we discussed the tradeoff between probability of detection and power efficiency. Yet higher probability of detection is in need for the improvement of sensing performance, collecting many samples to do so would not allow reducing power consumption. We will show that this tradeoff can be efficiently, in terms of probability of detection and power efficiency, alleviated by finding the optimal sensing time.

Recall the received data matrix (34) in a primary signal detection problem. Assume that we collect only n samples, where $1 \le n \le N$. We call this n a 'check point' of the sensing time. Then we select k antennas $(1 \le k \le K)$ which are assumed to be in a faded channel to shut down. Thus, after the checkpoint, there are only $K-k$ secondary antennas employed for $N-n$ samples.

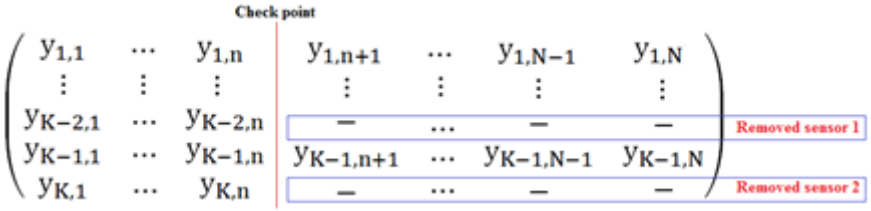

Fig. 6 Example of proposed scheme for K antennas and N samples

Fig. 6 shows an example of the received data matrix under this new scheme. After sensing n samples of K antennas, the system selects k antennas, which are considered to be more faded than others, to remove.

We have discussed that shutting down antennas with faded channel increases overall power efficiency. The detailed formulation of an equation on the efficiency of resources will be represented in the following subsection.

3.2.1 Efficiency of Resources

In this subsection, we present that removal of n numbers of antennas leads to deduction of resource usage. Recall the received data matrix Y (34). Assume that a power of $N \times p$ is required for each secondary users to have the antennas RF-chain switched on for the duration of the measurement and process it. Therefore, sensing using K antennas with N samples takes $K \times N \times p$ in power.

Consider a case of shutting down one antenna $(\mathrm{k} = 1)$, after n samples of sensing; this saves $(\mathrm{N} - \mathrm{n}) \times \mathrm{p}$ in power. Thus, if k antennas are chosen to be shut down after n samples of sensing, we save $\mathrm{k} \times (\mathrm{N} - \mathrm{n}) \times \mathrm{p}$ in power compared to that collect all N data samples for K antennas.

Power efficiency is proportional to the energy saved during the sensing process by shutting down antennas. That is, power efficiency should be an indicator of how much energy could be saved compared to the sensing of whole samples of all antennas. Therefore, we may represent the power efficiency η as follows.

$$\eta(n,k) = \frac{k \times (N-n)}{K \times N} \tag{35}$$

For example, in the case within the number of shutting down antennas is fixed into 1 (k = 1), the power efficiency η(n) becomes

$$\eta(n,1) = \frac{(N-n)}{K \times N} \tag{36}$$

We should note that this efficiency represents power efficiency, or network efficiency, as a certain amount of power is required for each secondary user to send the signal measurement. By shutting $\mathrm{K} - \mathrm{k}$ antennas down, we can improve the efficiency of power compared to sensing whole N sampling time series.

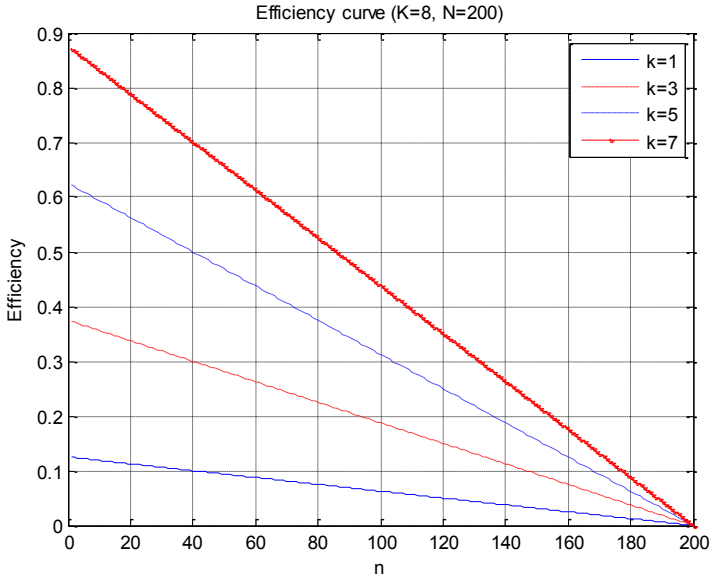

Fig. 7 Efficiency curve ($K = 8, N = 200$)

Fig. 7 shows power efficiency η(n) under K = 8 and N = 200 with varied k values. As this figure shows, upper equation of efficiency has bigger values as more number of antennas k is removed. Also for a given number of k, the efficiency is improved when less number of samples n is employed before the check point. As we have seen in the previous section, however, probability of detection increases when more number of samples is employed. Probability of detection has a tendency to increase when the bigger number of n is employed. Since we face with this tradeoff, we will discuss on finding optimum sensing time of CR network in the next section.

3.3 Optimum Sensing Time

Our aim of this thesis is to derive the target function of the CR system. The existence of an optimal sensing time is expected, that jointly maximizes the probability of detection and minimizes power consumption under given parameters. As there is a tradeoff between the probability of detection and power efficiency, the target function in this thesis is defined as

$$J(n,k) = (1-\alpha) \times P_d + \alpha \times \eta(n,k) \tag{37}$$

where $0 \leq \alpha \leq 1$. P_d is proportional to the number of sensing samples N, while $\eta(n,k)$ decreases as more number of samples are employed; thus, the constant α controls the overall level of this target function as well as it controls this target function to have a maximum point.

The tradeoff between two standards can be explained as followings.

(i) $\alpha \to 0$; The detection performance is regarded as a more important factor.

(ii) $\alpha \to 1$; Power efficiency is regarded as more important than the performance.

One notices that there may exist some range for α which keeps the target function into a function in which the optimal sensing time could be found. It would be varied by other parameters, such as probability of false alarm, the size of the data matrix, and so on.

Another focus to be set in this target function is how to obtain P_d. In this target function, the threshold value to calculate P_d is obtained by fixing P_f. From the equation (19), the threshold ε is defined as

$$\varepsilon = \left(\frac{Q^{-1}(P_f)}{\sqrt{N}} + 1 \right) \sigma_u^2 \tag{38}$$

Therefore, by using this target function, we can obtain the optimum value of check point, n, for different channel models. Also, we can conclude the optimal number of shut-down antennas for given number of check point and matrix size.

3.4 Antenna Selection

In this section, we discuss the antenna selection schemes employed in this thesis. Also, the worst case simulation criteria to compare with these selection schemes will be shown.

3.4.1 The Antenna with the Highest Signal Strength

In this thesis, the antenna selection scheme is performed for the channel where primary users are present. The sensing is performed to select the dedicated antenna, and the only selected antennas keep track of the activity of primary users in the dedicated sensing phrase.

By utilizing the fact that CR nodes involved in the spectrum sensing can measure the signal strength of active primary user signals, the proposed scheme selects the antennas with the highest signal strength as a dedicated antenna for the specified channel [16]. That is, the selected CR antenna has the highest signal strength among involved antennas. This scheme requires additional feedback information to report the signal strength for selecting the dedicated antenna.

3.4.2 Random Antenna Selection

The worst case is considered as a benchmark to compare criterions of removing antennas. In this case, antennas to remove are randomly selected, and overall performance is compared with other criterions.

Chapter 4

Numerical Results and Discussions

In this chapter, we present numerical results of the proposed scheme for the CR system. As mentioned, we assume Rayleigh fading channels for modeling multipath fading environments.

4.1 Non-Fading Channel

In this section, we consider the cases of non-fading channel to investigate the relationships between system parameters and numerical results. The target function is obtained from the approximate expressions of probability of detection (17) and false alarm (15). Because this simulation is based on the formulas, the antenna to shut down was randomly chosen. Therefore, this might be considered as the worst case simulation over non-fading channels. We set the SNR is equal to -10 dB, and probability of false alarm is set into 0.1.

4.1.1 Effects of Weighting Factor α

To investigate the effects of weighting factor α, size of the received data matrix is fixed while α is varied. First we consider the case of received data matrix size 2× 400, where two antennas are receiving signals and overall sensing period is 400.

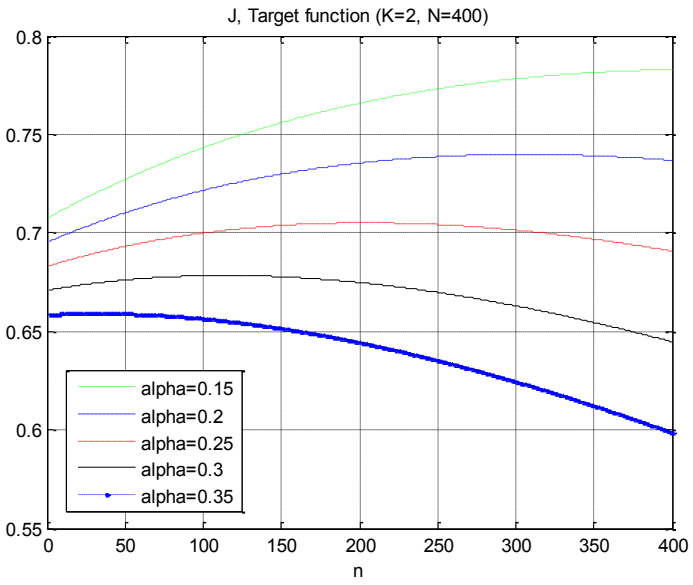

Fig. 8 Target function over non-fading channels ($\boldsymbol{K = 2, N = 400,\ P_f = 0.1}$)

Fig. 8 illustrates the target function performance under various range of α. When α is set into a relatively smaller value, the target function tends to have bigger value overall; this is because the slope of efficiency function $\eta(n, k)$ is much steeper than the one of P_d curve. It is also notable that the target function does not always have a point whose derivative is 0 therefore the optimum check point exists only within the constrained ranged of α.

As we can see from here, optimization of the target function, or to find the optimum sensing time exists under certain range of α. In Fig. 8 we can also observe that the optimum check point which maximizes the target function tends to have lower value as α gets bigger. Larger α decreases the overall portion of detection probability of the target function. Therefore, it is natural in this case the optimal sensing time n is relatively a smaller number to maintain a certain level of detection probability for maximizing the target function. This can be re-listed as follows;

(i) α → 0; since the detection performance is regarded as more important factor, more number of samples are favorable to maximize the target function.

(ii) α → 1; power efficiency is considered more significant than the detection performance. Therefore the sooner antennas shut down, the higher value of the target function is achieved.

4.1.1.1 Meaningful Range of α

Because the target function has a maxim point only within a certain range of α, it is necessary to figure out the meaningful range of α. We present the results of the target functions with altered α. In Fig. 8, we observed that with α value of 0.15, the target function does not have a maximum point, rather it keeps increasing. On the other hand, with bigger α values, the target functions have points which maximize them. In Fig. 9, the case with bigger α is considered with same other parameters.

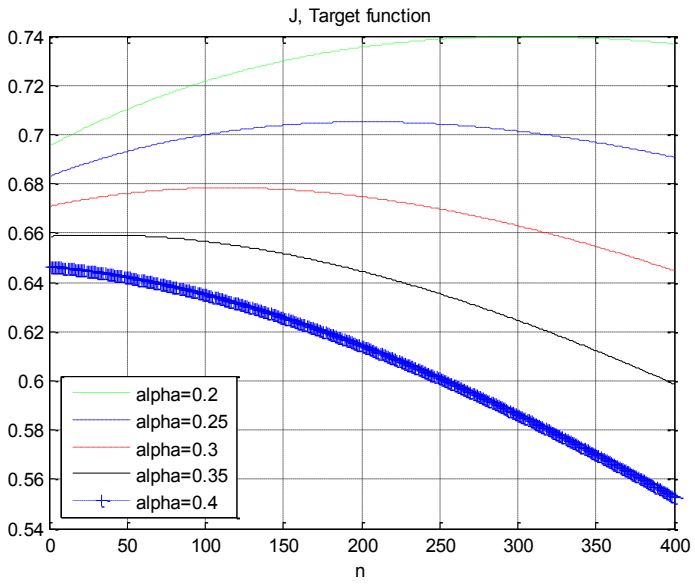

Fig. 9 Target function over non-fading channels for different α values

The target function has a maximum point except the case of $\alpha = 0.4$. Therefore, we can conclude that under the given condition, the meaningful range of α roughly lies on between 0.2 and 0.35. As in this case, meaningful range of α is varied depending on the parameters used in the simulation. Those further parameters and their effects are discussed in the next subsections.

4.1.2 Effects of Sensing Time

Another case is simulated based on more number of time series samples with a same number of antennas. Fig. 10 illustrates the target function with two antennas and doubled sensing time.

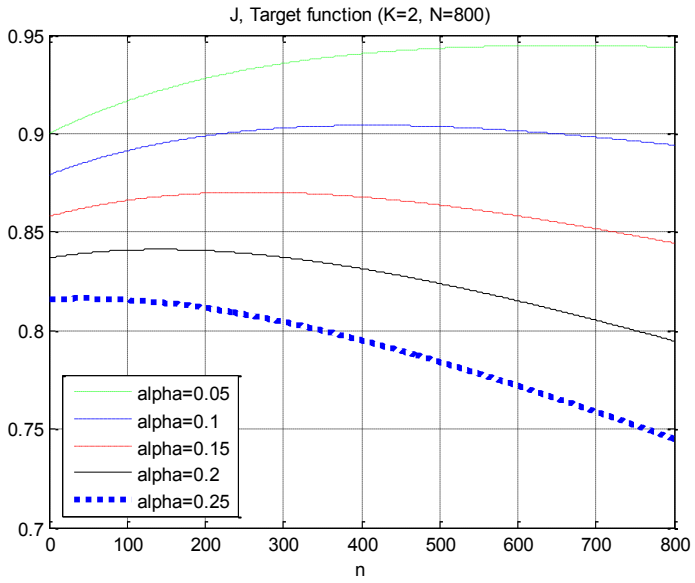

Fig. 10 Target function over non-fading channels ($K = 2, N = 800, P_f = 0.1$)

Both the probability of detection and efficiency function got changed as more numbers of time series samples are employed. Fig. 11 and Fig. 12 are the figures of detection probability and efficiency function. Comparing figures 5 and 11, as expected, probability of detection is increased as many samples are adopted and the slope of efficiency function gets less steeper compared to the case of 400 samples.

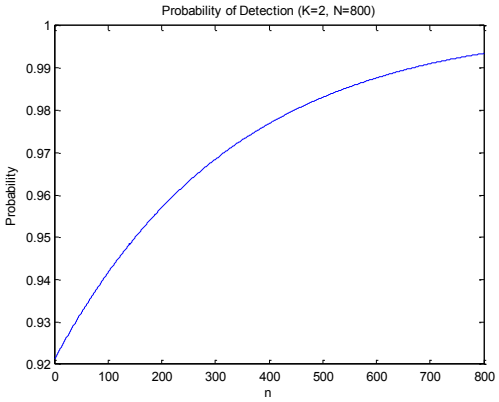

Fig. 11 Detection probability over non-fading channels ($K = 2, N = 800$, $P_f = 0.1$)

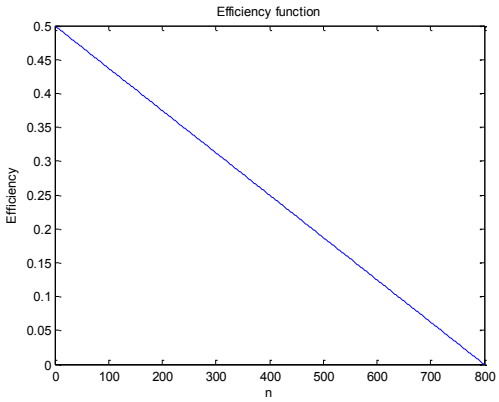

Fig. 12 Efficiency function curve ($K = 2, N = 800, P_f = 0.1$)

Due to this change, the range of α to fix the target function to have a maximum point is altered. The meaningful range of α , in this case, is in between 0.05 and 0.25, as in Fig. 10. Another notable thing yielded by these changes is overall level of the target function. Compared to the case of $N = 400$, we can find that the overall level of the target function is highly increased.

4.1.3 Effects of the Number of Antennas

Consider now the case when there is one more antenna with same parameters.

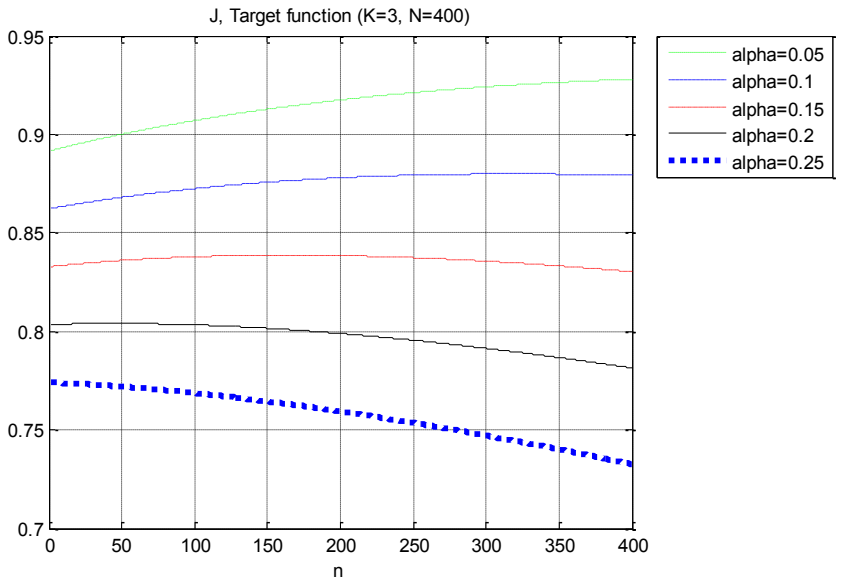

Fig. 13 Target function over non-fading channels ($K = 3, N = 400, P_f = 0.1$)

Fig.13 illustrates a case with three antennas employed under the same conditions. As the number of antennas increases, the optimum sensing time decreases. Thus, it is considered better from the view of power efficiency and detection performance to shut down an antenna earlier when we adopt more number of antennas. Under this condition, the meaningful range of α exists between 0.1 and 0.2.

4.1.4 Effects of False Alarm Probability

Fig. 14 shows the target function under non-fading channel when the false alarm probability is set into 0.2.

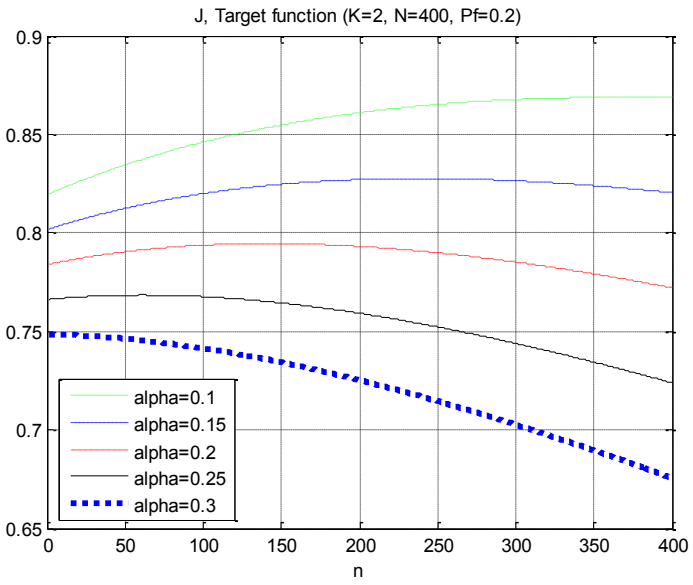

Fig. 14 Target function over non-fading channels($K = 2, N = 400, P_f = 0.2$)

As we have seen in the previous section and in Fig. 2, the increase of false alarm probability means lower value of threshold. Because of this reason, probability of detection is increased as well. The overall rise of the target function is also due to this reason. Under this condition, the meaningful range of α exists between 0.1 and 0.25.

Table 1 Comparison of target function over non-fading channels

α	K = 2 N = 400 P_f = 0.1		K = 2 N = 800 P_f = 0.1		K = 3 N = 400 P_f = 0.1		K = 2 N = 400 P_f = 0.2	
	Max. J	Opt. n	Max. J	Opt. n	Max. J	Opt. n	Max. J	Opt. n
0.05	-	-	0.944	656	-	-	-	-
0.1	-	-	0.904	413	0.879	318	0.868	369
0.15	-	-	0.870	260	0.838	163	0.827	239
0.2	0.739	305	0.841	143	0.804	45	0.794	141
0.25	0.705	204	0.816	45	-	-	0.768	61
0.3	0.678	114	-	-	-	-	-	-
0.35	0.659	32	-	-	-	-	-	-
Meaningful range of α	0.2 ~ 0.35		0.05 ~ 0.25		0.1 ~ 0.2		0.1~0.25	

Table 1 summarizes comparison between simulation results on variables which we consider and the meaningful range of α for each

case. Max. J indicates a maximum point of the target function J, and Opt. n indicates the optimum sensing time n.

The results of searching for meaningful range of α demonstrate that when more number of samples are given, smaller α is required for the target function J, owing to the fact that increase of the number of samples yields improvements on the overall level of probability of detection.

4.2 Fading Channel

In this section, we investigate the performance of proposed sensing selection methods under various conditions. We compare the results obtained from the simulations of antenna selection schemes and the random antenna selection scheme. As previously discussed, the worst case simulation is based on the case where the removing antennas are chosen randomly. If the performance of the case which is employing the suggested criteria overwhelms that of random selection of antennas, it can be seen that the suggested criterion is creditable to use.

Like previous examinations, we assume that there are two antennas and each antenna collects 400 samples during the sensing time.

A fundamental parameter determining the quality of detection is the average SNR, which mainly depends on the primary user's transmitted power as well as its distance to the secondary users. Since our goal is to achieve optimum sensing time over the proposed antenna selection method, let us set the two scenarios of average SNR. In the first scenario, the averages SNR of two antennas have big differences. In the second scenario, the average values of two antennas are similar. The first scenario shows an environment in which one antenna is experiencing rather severe fading, while another one is in a better condition. The second scenario shows an environment where two antennas are under similar but slightly different average SNRs.

We set α value into the range of 0.15 to 0.35. Also, probability of false alarm is set into 0.1.

4.2.1 Channels with No Correlations Assumed

In this subsection, we model and compare the results of the Rayleigh fading channel assuming that there are no correlations in temporal and frequency domains.

4.2.1.1 Channels with Distinguished Average SNR

In this section, we proceed to show the numerical results of the scenario where one antenna is under 3 dB of average SNR, while another is under -17 dB of average SNR.

4.2.1.1.1 Worst Case Simulation

Fig. 15 illustrates the detection probability when the average SNR over two antennas have relatively big differences. The noticeable difference compared to the previous simulations on non-fading channel lies on the fact that detection probability can be approximated 1 at $n \cong 130$ as the number of samples n increases. This is due to the fact that the average SNR assumed in this simulation $(\bar{\gamma} = 3\ dB, -17\ dB)$ is improved compared to the assumption we used in the non-fading channels$(\bar{\gamma} = -10\ dB)$. We obtain highly improved detection probability that it reaches 0.9 at $n = 44$. This will be compared with the results from other selection methods.

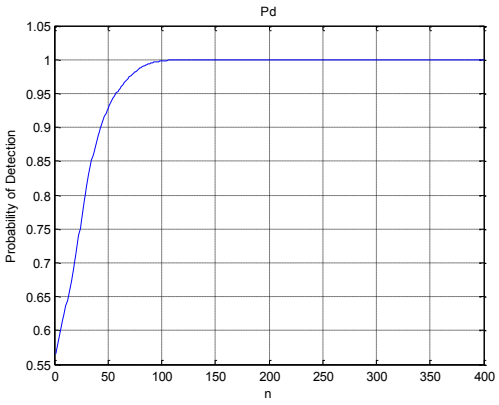

Fig. 15 Detection probability over Rayleigh fading channels for the random antenna selection $(\bar{\gamma} = 3\ dB, -17\ dB)$

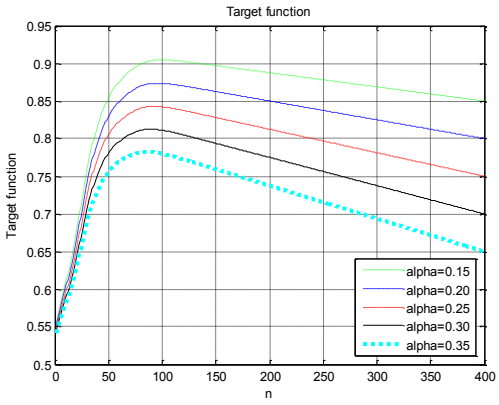

Fig. 16 Target function over Rayleigh fading channels for the random antenna selection $(\bar{\gamma} = 3\ dB, -17\ dB)$

Subsequently, the target function in Fig. 16 has its peak point followed by linear drop.

The upper simulations are based on the case that the average SNR of two antennas has big difference each other. The average SNR of one antenna was fairly good, where another one was under a bad condition.

4.2.1.1.2 Selection Based on Signal Strength

In this subsection, we investigate simulation results of the selection based on the signal strength. Fig. 17 illustrates the curve of detection probability. The average SNRs are fixed as same as the previous simulation; 3 dB and -17 dB respectively for two antennas. We observe that the detection probability has much higher value even before it saturates approximately to 1 compared to the worst case, not to mention that it saturates earlier. To specify, the saturation point under this scheme is at $n \cong 50$, and the detection probability reaches 0.9 at $n = 12$.

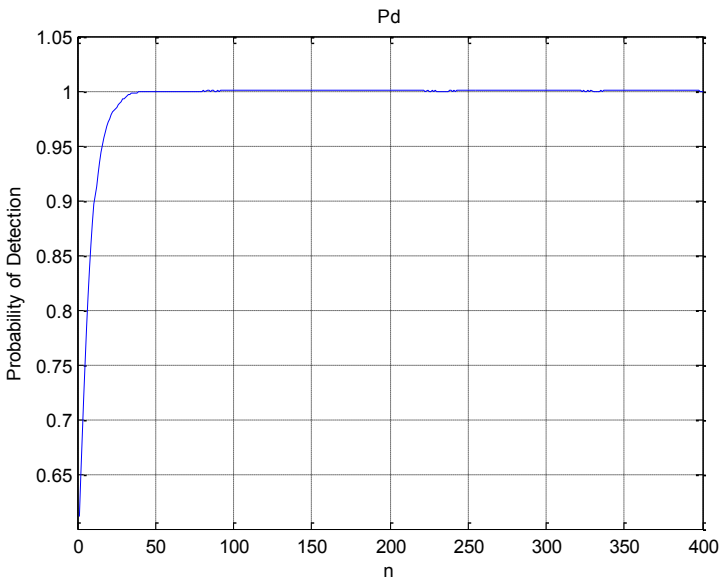

Fig. 17 Detection probability over Rayleigh fading channels for the proposed selection method ($\overline{\gamma} = 3\ dB, -17\ dB$)

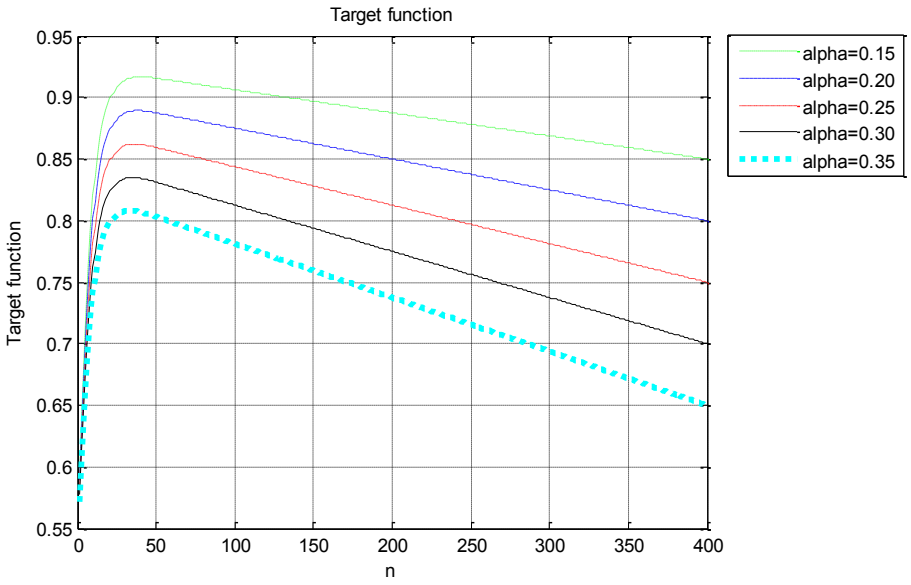

Fig. 18 Target function over Rayleigh fading channels for the proposed selection method ($\bar{\gamma} = 3\ dB, -17\ dB$)

Fig. 18 depicts the target function over Raleigh fading channels for the proposed selection scheme. It is noticeable that the overall level and maximum points of target functions are higher than those of the worst case simulation, as shown in Fig. 18 and Fig. 16. The target function for this antenna selection scheme reaches its maximum point much earlier than one of worst case. The detailed comparisons of the target function from different selection schemes are shown in Table 2.

Table 2 Comparison of target function over Rayleigh fading channels ($\bar{\gamma} = 3dB, -17dB$)

α	Worst case simulation			Selection based on signal strength		
	J when $P_d = 0.9$	Max. J	Opt. n	J when $P_d = 0.9$	Max. J	Opt. n
0.15	0.8343	0.9045	100	0.8479	0.9168	40
0.2	0.8114	0.8735	95	0.8265	0.8894	38
0.25	0.7885	0.8429	91	0.8052	0.8622	37
0.3	0.7656	0.8126	88	0.7839	0.8351	35
0.35	0.7427	0.7825	86	0.7625	0.8081	34

Clearly, we see that the selection method based on the signal strength drives improvements. Not only the target function reaches its maximum point earlier but also it achieves higher performance.

Also, the target function achieves the higher value while maintaining 0.9 of detection probability; that is, using this selection method enables the system to shut down much earlier than the random antenna selection scheme. By doing so, the overall energy efficiency is increased maintaining this improved detection probability.

4.2.1.2 Channels with Similar Average SNR

To compare the previous simulations of another scenario where the two antennas are under similar fading, we construct a case with two antennas, whose average SNR are -4 dB and -7 dB respectively.

4.2.1.2.1 Worst Case Simulation

The probability of detection over Rayleigh fading channel for the random antenna selection scheme has been shown in Fig. 19. As depicted in this figure, the detection probability under this condition underperforms that of previous simulation which assumed that there are big differences between antennas.

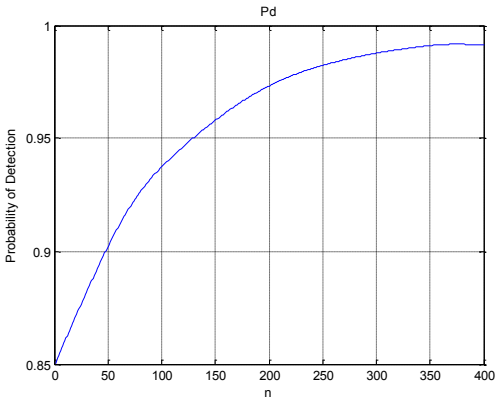

Fig. 19 Detection probability over Rayleigh fading channels for the random antenna selection ($\bar{\gamma} = -4\ dB, -7\ dB$)

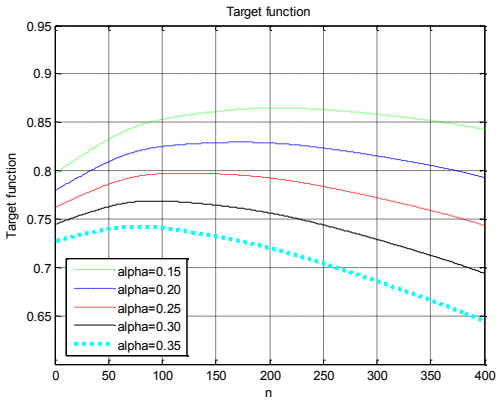

Fig. 20 Target function over Rayleigh fading channels for the random antenna selection ($\bar{\gamma} = -4\ dB, -7\ dB$)

The simulated target function results are depicted in Fig. 20. Unlike the previous case, the performance of the target function is not a linear function after its peak point; rather each of the target functions has an optimum sensing time.

Compared to the scenario where the two antennas have big differences, results suggest a significant loss in terms of detection probability. We observed that when only one channel is deeply faded, it is more likely to have a much better performance on detection probability even we select one antenna to remove randomly. However, when two channels are moderately faded with similar amount, the detection probability performance is significantly degraded.

4.2.1.2.2 Selection Based on Signal Strength

The following Fig. 21 and Fig. 22 depict the probability of detection and the target function with the same conditions but average SNR of -4 dB and -7 dB respectively.

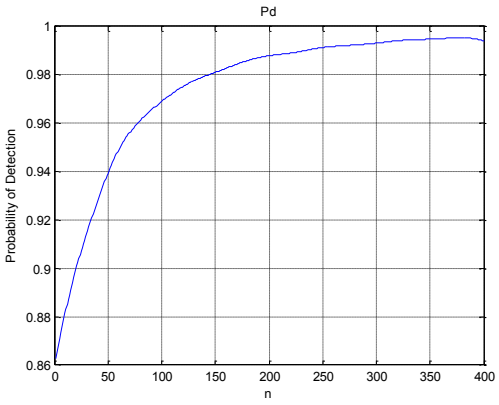

Fig. 21 Detection probability over Rayleigh fading channels for the proposed selection method ($\bar{\gamma} = -4\ dB, -7\ dB$)

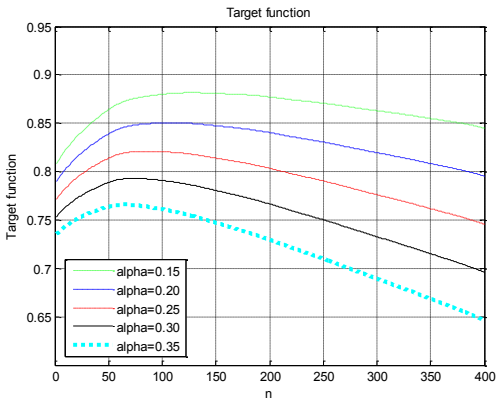

Fig. 22 Target function over Rayleigh fading channels for the proposed selection method ($\bar{\gamma} = -4\ dB, -7\ dB$)

As expected, selection based on signal strength improves the performance of detection, compared to the worst case simulation for the same level of average SNRs (shown in Fig. 19 and Fig. 20). Both the detection probability and the target function showed increase through its overall range. In the case of detection probability, it reaches 0.9 at $n = 21$ when the antennas are selected based on signal strength; however, when selected randomly, the detection probability reaches 0.9 at $n = 48$. This indicates that more than half of the sensing time and energy can be saved with this scheme. The

detailed comparison of the target functions in Fig. 20 and Fig. 22 is illustrated in Table 3.

Table 3 Comparison of target function over Rayleigh fading channels ($\bar{\gamma} = -4\ dB, -7\ dB$)

α	Worst case simulation			Selection based on signal strength		
	J when $P_d = 0.9$	Max. J	Opt. n	J when $P_d = 0.9$	Max. J	Opt. n
0.15	0.8311	0.8648	208	0.8369	0.8816	127
0.2	0.8081	0.8294	173	0.8155	0.8504	110
0.25	0.7851	0.7973	120	0.7942	0.8209	86
0.3	0.7621	0.7688	92	0.7728	0.7930	73
0.35	0.7391	0.7421	77	0.7515	0.7659	66

It has been shown in the comparison that a higher level of the target function can be achieved by employing the proposed selection scheme, as well as the optimum sensing point can be efficiently shortened. The effectiveness of the proposed scheme becomes more obvious when the weighting factor α has smaller value.

We conclude that antenna selection based on signal strength contributes to improvement on the performance over coherent Rayleigh channels, as the both two case simulations for the antenna selection based on received signal strength is outperform the performance those of the worst case simulation.

Furthermore, under the circumstances in which some channels are experiencing severe fading compared to others, the proposed antenna selection scheme particularly shows more achievements; not only higher detection probability can be obtained, the system maintains desirable power efficiency.

4.2.2 Channels with Correlations: AR Modeling

In this section, we compare random antenna selection scheme and the proposed antenna selection method in AR-modeled Rayleigh fading channels.

AR modeling and its results on generating channel fading would be greatly varied upon the orders of the AR model, maximum Doppler frequency, the symbol frequency, and so on. The filter length to generate the channel coefficients, also, has a significant role to decide how much the channel is faded.

In this thesis, we have employed maximum Doppler frequency of 150Hz, symbol frequency of 3ksps. In the filter, the first p samples are ignored, where p denotes the order of AR model. Over many observations on simulations, we decided to employ AR(50) model as it is qualified to provide more proper conditions for this thesis research.

4.2.2.1 Channels with Distinguished Average SNR

In this subsection, we illustrate the worst case simulation results over different orders of AR-modeled Rayleigh fading channels to compare them. We also present the performance over AR(50) modeled Rayleigh fading channels when the average SNR values are distinguished each other.

4.2.2.1.1 Worst Case Simulation

First, we investigate the worst case simulation under AR(100) modeled Rayleigh fading as a comparison with AR(50) modeled Rayleigh fading.

Fig. 23 and Fig. 24 show the detection probability and the target function over AR(100) modeled Rayleigh channels for different values of weighting factor α. The average SNR of 3 dB and -17 dB are used for two antennas respectively.

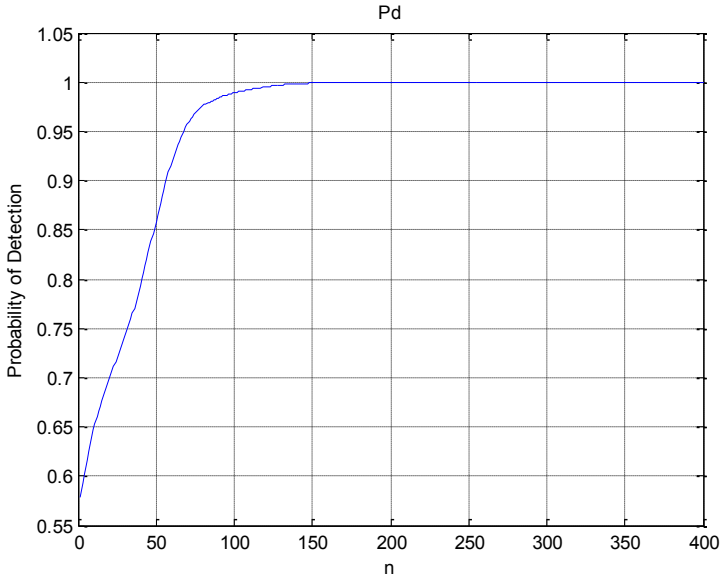

Fig. 23 Detection probability over AR(100) modeled Rayleigh fading channels for the random antenna selection ($\bar{\gamma} = 3\ dB, -17\ dB$)

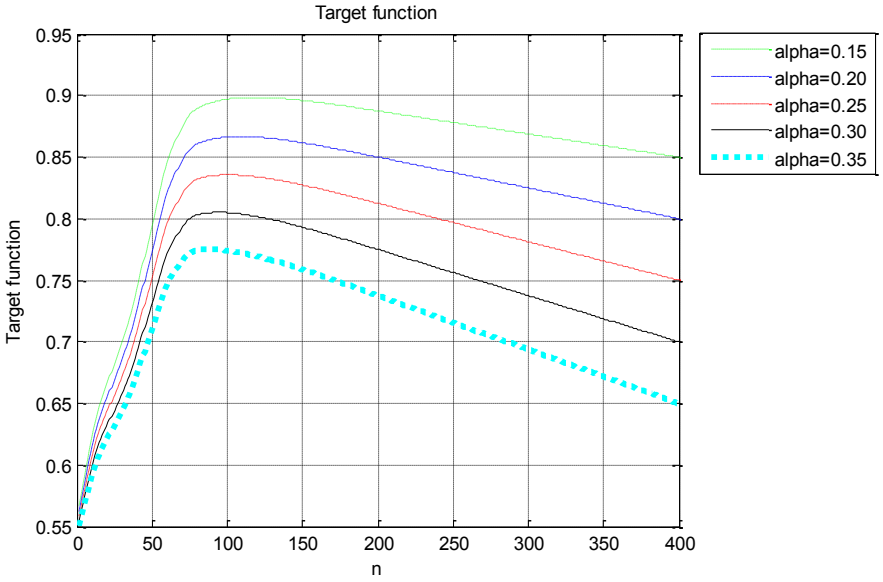

Fig. 24 Target function over AR(100) modeled Rayleigh fading channels for the random antenna selection ($\bar{\gamma} = 3\ dB, -17\ dB$)

From Fig. 23, one sees that detection probability saturates at $n \cong 200$. Also, from Fig. 24, one notes that the optimum sensing time under this condition exist around $n = 100$.

Table 4 Worst case simulation over AR(100) modeled Rayleigh fading channels ($\bar{\gamma} = 3\ dB, -17\ dB$)

α	Maximum point of J	Optimum sensing time n
0.15	0.8984	122
0.2	0.8667	107
0.25	0.8356	101
0.3	0.8051	94
0.35	0.7752	88

Table 4 illustrates the simulation results under AR(100) modeled Rayleigh fading. We compare this results with the ones of AR(50) modeled Rayleigh fading. Fig. 25 and Fig. 26 show the detection probability and the target function in AR(50) modeled Rayleigh fading channels.

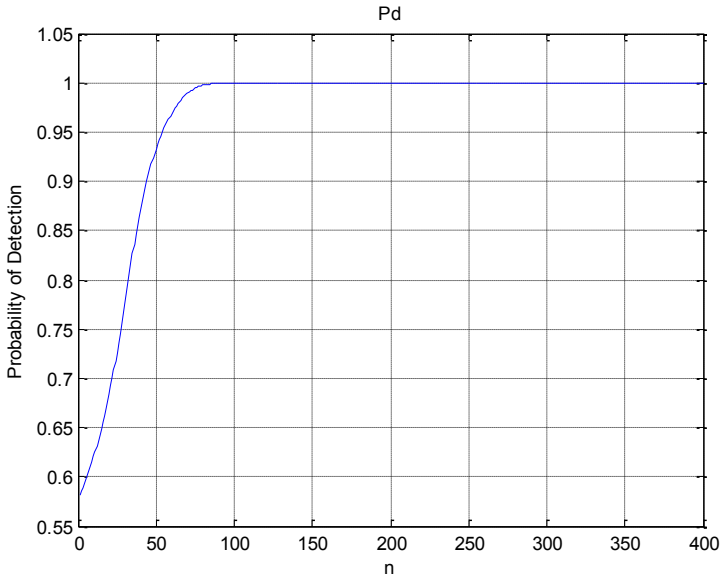

Fig. 25 Detection probability over AR(50) modeled Rayleigh fading channels for the random antenna selection ($\bar{\gamma} = 3dB, -17dB$)

The average SNR values are 3 dB and -17 dB for two antennas. The detailed comparison of AR-modeled Rayleigh fading channels is shown in Table 4. The detection probability reaches its saturation point earlier than that in AR(100) modeled Rayleigh fading channels.

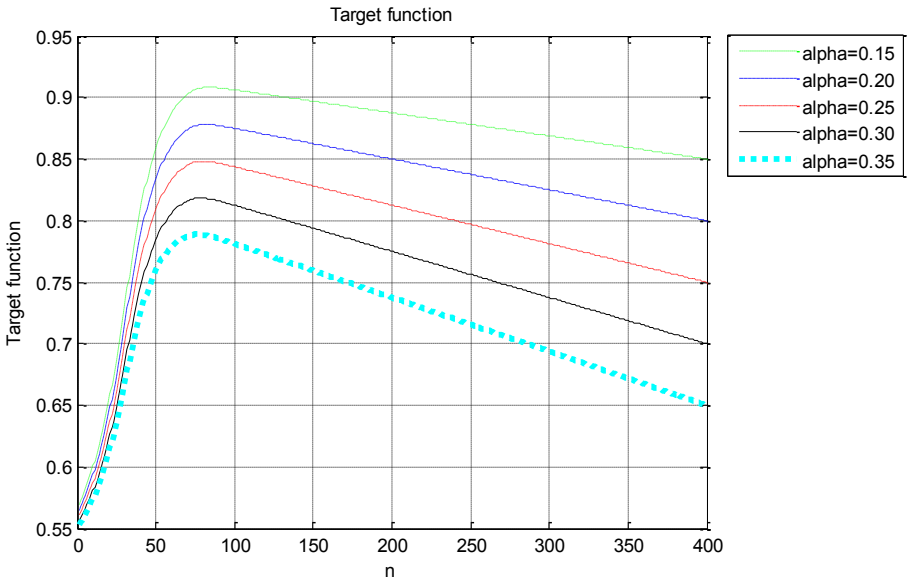

Fig. 26 Target function over AR(50) modeled Rayleigh fading channels for the random antenna selection ($\bar{\gamma} = 3\ dB, -17\ dB$)

Also, from Fig. 26, the target function achieves higher maximum point than AR(100) modeled Rayleigh fading channel, as illustrated in Table 4. Therefore, the optimum n decreases when the order of the AR model decreases; as expected, one can achieve better performance using less samples.

We have adopted AR(50) model for the rest of our experiments because its performance is close to that of simulations on the channels without correlations as shown in Fig. 25 and Fig. 15. Also, lower-order AR processes have been reported to not provide a good match to the desired band limited correlation statistics [15].

4.2.2.1.2 Selection Based on Signal Strength

Up to this point, we have dealt with random selection of antennas, or the worst case simulation, where the antennas experience AR-modeled Rayleigh fading. We also made a comparison between different scenarios; one scenario where the values of average SNRs have big differences and another one where they are more similar. Intuitively, the performance of the latter scenario underperforms the one of the former scenario. Moreover, random selection will degrade this performance of sensing even more. This is due to the fact that under random selection method even such antennas with

strong average SNR are likely to be selected and shut down. In this subsection, further simulation results for the selection based on signal strength are provided.

We consider the case where the average SNR values are set into 3 dB and -17 dB. The probability of detection has been plotted in Fig. 27.

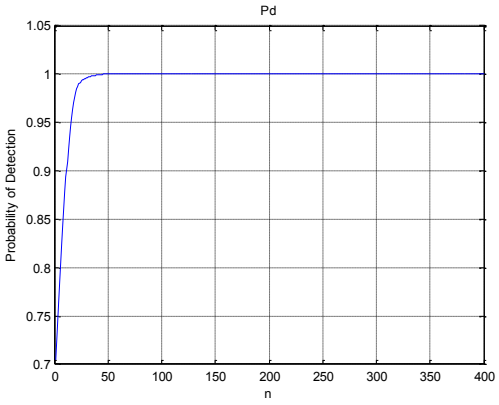

Fig. 27 Detection probability over AR(50) modeled Rayleigh fading channels for the antenna selection based on signal strength ($\bar{\gamma} = 3\ dB, -17\ dB$)

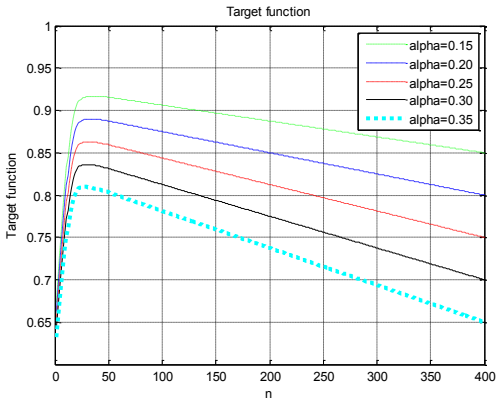

Fig. 28 Target function over AR(50) modeled Rayleigh fading channels for the antenna selection based on signal strength ($\bar{\gamma} = 3\ dB, -17\ dB$)

As expected, selection based on signal strength improves the performance of detection in this case. In the worst case simulation, detection probability saturates at $n \cong 120$ and it reaches 0.9 at $n = 45$. On the other hand, when the antennas are selected according to its received signal strength, detection probability saturates at $n = 49$ and reaches 0.9 at $n = 12$. Clearly, the latter selection method enables users to obtain higher detection probability. This positive effect can be also observed when we compare the target function illustrated in Fig. 28 with Fig. 26.

Table 5 presents the comparison between the target functions obtained from previous simulations.

Table 5 Comparison on target function over AR(50) modeled Rayleigh fading channels ($\bar{\gamma} = 3\ dB, -17\ dB$)

α	Worst case simulation			Selection based on signal strength		
	J when $P_d = 0.9$	Max. J	Opt. n	J when $P_d = 0.9$	Max. J	Opt. n
0.15	0.8365	0.9082	83	0.8456	0.9169	39
0.2	0.8134	0.8781	82	0.8244	0.8896	35
0.25	0.7903	0.8482	80	0.8031	0.8628	30
0.3	0.7672	0.8184	78	0.7819	0.8362	28
0.35	0.7441	0.7887	77	0.7607	0.8097	27

We observe from this table that for a given condition, selection based on signal strength will be needed to deliver improved performance. The results shown in Fig. 28 suggest that antenna selection based on signal strength is more effective than random selection in that the maxima of the target function is increased for all given α and the optimum sensing time n can be decreased as well.

4.2.2.2 Channels with Similar Average SNR

In this subsection, we present the numerical results of detection performance, when the channel is modeled into AR(50) Rayleigh fading and the average SNR values are similar to each antenna.

4.2.2.2.1 Worst Case Simulation

Fig. 29 and Fig. 30 depict the detection probability and the target function as a function of the sensing time, n, under AR(50) modeled Rayleigh fading ($\bar{\gamma}$ = -4 dB and -7 dB for two antennas) for different α values. The decision threshold is modified such that $P_f = 0.1$. The channel to be shut down is chosen randomly.

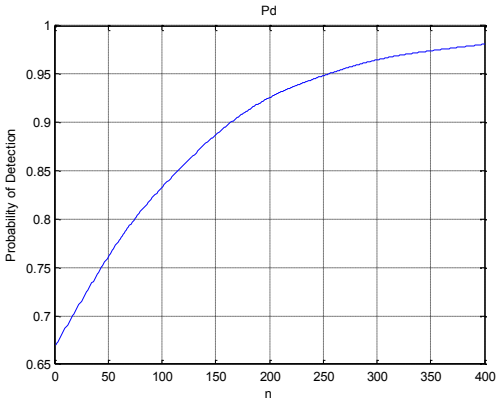

Fig. 29 Detection probability over AR(50) modeled Rayleigh fading channels for the random antenna selection ($\bar{\gamma} = -4\ dB, -7\ dB$)

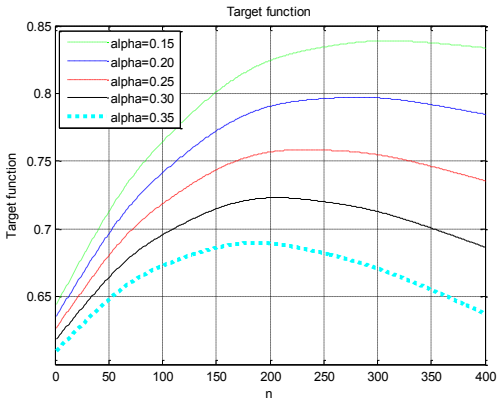

Fig. 30 Target function over AR(50) modeled Rayleigh fading channels for the random antenna selection ($\bar{\gamma} = -4\ dB, -7\ dB$)

As seen in these figures, the detection probability is degraded significantly compared to the scenario where the two antennas have relatively different average SNRs. For comparison, we have also plotted Fig. 25 and Fig. 26.

Results indicate that sensing under similar fading has a significant negative impact on the detection performance when random selection is employed. The optimum sensing time and corresponding maximum point of the target function is shown in the following table 5. Those results will be compared with the ones from the selection based on signal strength.

4.2.2.2.2 Selection Based on Signal Strength

Fig. 31 provides a plot of detection probability versus the sensing time under AR(50) modeled Rayleigh fading when the average SNR values have smaller differences. The average SNRs of two antennas are -4 dB and -7 dB. For this curve, the decision threshold ε is chosen such that $P_f = 0.1$. Comparing to Fig. 27, the result indicates a significant degradation in terms of detection performance.

However, when we compare Fig. 31 with Fig. 29, we can discover that antenna selection based on signal strength cancels the deleterious impact of degraded overall average SNR effectively. For example, detection probability of the antenna selection method

based on the received signal strength reaches 0.9 at $n = 74$, while the one of the worst case simulation reaches 0.9 at $n = 165$.

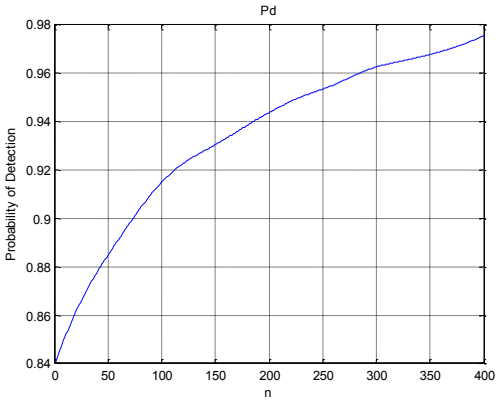

Fig. 31 Detection probability over AR(50) modeled Rayleigh fading channels for the antenna selection based on signal strength ($\bar{\gamma} = -4\ dB, -7\ dB$)

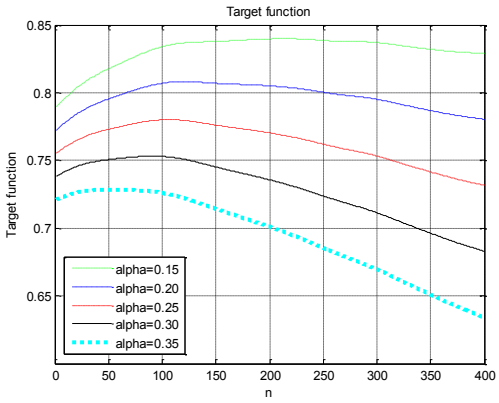

Fig. 32 Target function over AR(50) modeled Rayleigh fading channels for the antenna selection based on signal strength ($\bar{\gamma} = -4\ dB, -7\ dB$)

Comparing figures 32 and 30 for the same sensing time, as expected, there is an improvement of the performance when employing the antenna selection method based on signal strength in the scenario 2, where two antennas are more similar. The detailed comparison between these two figures is given in Table 6.

Table 6 Comparison on target function over AR(50) modeled Rayleigh fading channels ($\bar{\gamma} = -4\ dB, -7\ dB$)

α	Worst case simulation			Selection based on signal strength		
	J when $P_d = 0.9$	Max. J	Opt. n	J when $P_d = 0.9$	Max. J	Opt. n
0.15	0.8097	0.8389	310	0.8265	0.8399	214
0.2	0.7794	0.7972	282	0.8019	0.8082	120
0.25	0.7490	0.7584	232	0.7772	0.7801	106
0.3	0.7187	0.7230	206	0.7526	0.7532	91
0.35	0.6882	0.6896	187	0.7279	0.7283	49

As shown in this comparison table, the target function under the antenna selection method based on signal strength achieves higher maximum points for all weighting factors α. We also see that the optimum sensing point n can be much shortened by adopting this antenna selection method.

Thus, we conclude that the detection performance can be less affected by degraded overall average SNR when the antenna selection is based on signal strength.

Chapter 5

Conclusions and Future Work

This chapter concludes the main results achieved in this thesis. Some possible future research directions based on this thesis are discussed as well.

5.1 Conclusions

Spectrum sharing and access are important issues facing opportunistic communication in multiuser cognitive radio systems. In this thesis, we studied an optimum sensing time with the proposed antenna selection schemes as a means to improve the performance of sensing based opportunistic spectrum access under fading for the CR system.

User priorities pose unique design challenges that are not faced in conventional wireless systems. In an environment with multiple primary and secondary users, the tradeoff between detection performances and power efficiency exists. To characterize the tradeoff, we set up a target function which consists of the detection probability and power efficiency. Then we identify the optimum amount of sensing time that maximizes the target function.

The optimum check point is defined as the stop point for sensing which maximizes the target function between the probability of detection and power consumption. The proposed scheme on the antenna selection selects ones with the highest signal strength as the dedicated antenna for the channel where a primary user is active. This scheme is compared with a

worst case simulation, in which the antennas to be shut down are selected randomly.

Assumptions on the received data matrix are as follows; there are two antennas and the sensing time is 400. We first analyzed the results of altered variables under non-fading. The results from the non-fading channel simulations indicate that the weighting factor α has a meaningful range in the target function which largely depends on other parameters.

For the Rayleigh fading channels, two modeling techniques were considered. The first one is modeling coherent channels in which there is no correlation on temporal and frequency domains. The second technique is AR modeling which models the correlations on temporal and frequency domains. Over each fading channel the two selection methods are employed. For comparison, we have settled two scenarios for each selection method; scenario 1 where there exist big differences on the average SNR between antennas, and scenario 2 where there exist smaller differences between them. Compared to the scenario 2, scenario 1 provided the better performance results. It has one channel whose average SNR is in a good condition.

In a fading environment without correlations, the results of the scenario 1 where the two antennas have distinguishing average SNRs showed that the proposed selection criteria increased the maximum point of the target function up to 3%, in which the optimum sensing time was shortened into 40% of the worst case simulation. This is particularly important from the perspective of power efficiency. The results of the scenario 2 where the average SNRs are more similar showed comparable improvements on the performance enhancement of the target function. The optimum sensing time was shortened into 60% ~ 90% of the worst case simulation, which is a smaller improvement than in the first scenario. Also, the effectiveness of the proposed selection criteria got lowered as the weighting factor α increased.

In a fading environment with correlations on temporal and frequency domains, the results of scenario 1 showed that the proposed selection criteria increased the maximum point of the target function up to 3% in which the optimum sensing time was shortened into 35% ~ 47% of the worst case simulation. The results of scenario 2 showed up to 6% of

improvement on the maximum points of the target functions. The optimum sensing time using the proposed selection criteria was shortened into 26% ~ 70% of that of the worst case simulation. The effectiveness of the proposed selection criteria gets better as the weighting factor α increased.

The results indicate that in both Rayleigh fading models, the proposed criteria can provide enhancements to both detection performance and power efficiency. When the channel is modeled as Rayleigh fading without correlations, the performance is more stable with less variation. Especially in the scenario 1, the improvements on the performance are flat for different α values. Therefore, we can conclude that the proposed selection scheme may yield more stable and expected improvements when the channels have different average SNR. This is due to the white Gaussian noise added in the process of AR modeling.

Using the antenna selection scheme based on signal strength we have proved that there indeed exists an optimal sensing time which achieves the best tradeoff. Computer simulations have shown that for two Rayleigh fading models and two different scenarios for average SNRs, the target function achieves higher value while maintaining 90% detection probability when the proposed antenna selection criteria is employed. The optimal sensing time decreases up to 26% at most compared to the worst case simulation.

5.2 Possible Future Work

While we studied the optimum check point and the antenna selection methods over fading channels, more research needs to be done to develop efficient antenna selection schemes and methods to optimize performance in such a setting. In a fading environment with correlations, the performance under the scenario where the average SNRs of antennas are more similar is varied by which weighting factor is employed. In such a scenario, an optimum weighting factor is yet to be found. In other words, through more observations and mathematical verifications, it would be possible to find the optimum weighting factor for this scenario.

It is well-known that the energy detector's performance is susceptible to uncertainty in noise power [26]. In such cases, alternative detection schemes such as cyclic feature detection [27] may be employed. Performance analysis of spectrum sensing in this case can be the subject of future research.

References

[1] D. D. Ariananda, M. K. Lakshmanan and H. Nikoo, "A survey on spectrum sensing techniques for cognitive radio," *Second International Workshop on Cognitive Radio and Advanced Spectrum Management*, pp. 74-79, May 2009.

[2] National Telecommunications and Information Administration (NTIA), "FCC Frquency Allocation Chart," available at http://www.ntia.doc.gov/osmhome/allochrt.html 2003.

[3] J. Mitola, *Software Radio Architecture*, John Wiley & Sons, New York, NY, USA, 2000.

[4] S. Srinivasa and S. A. Jafar, "Cognitive radio networks: how much spectrum sharing is optimal?," *IEEE Global Telecommunications Conference*, pp. 3149-3153, November 2007.

[5] H. Urkowitz, "Energy detection of unknown deterministic signals," in *Proceedings of the IEEE*, vol. 55, no. 4, pp. 523-531, April 1967.

[6] Y. Chen, "Optimum number of secondary users in collaborative spectrum sensing considering resources usage efficiency," *IEEE Communications Letters*, vol. 12, no. 12, pp. 877-879, December 2008.

[7] F. F. Digham, M.-S. Alouini, and M. K. Simon, "On the energy detection of unknown signals over fading channels," *IEEE International Conference on Communications*, vol. 5, pp. 3575-3579, May 2003.

[8] P. Kaligineedi and V. K. Bhargava, "Distributed detection of primary signals in fading channels for cognitive radio networks," *IEEE Global Telecommunications Conference*, pp. 1-5, December 2008.

[9] Y. Zeng, Y.-C. Liang, A. T. Hoang, and R. Zhang, "A review on spectrum sensing techniques for cognitive radio: challenges and solutions," *EURASIP Journal on Advances in Signal Processing*, no. 2, pp. 1-15, October 2009.

[10] S. M. Kay, *Fundamentals of Statistical Signal Processing: Detection Theory*, Prentice Hall, Upper Saddle River, NJ, USA, 1998.

[11] Y.-C. Liang, Y. Zeng, E. Peh, and A. T. Hoang, "Sensing-throughput tradeoff for cognitive radio networks," *IEEE Transactions on Wireless Communications*, vol. 7, no. 4, pp. 1326-1337, June 2007.

[12] D.-C. Oh, and Y.-H. Lee, "Energy detection based spectrum sensing for sensing error minimization in cognitive radio networks," *International Journal of Communication Networks and Information Security*, vol. 1, no. 1, pp. 1-5, April 2009.

[13] S. M. Kay, *Modern Spectral Estimation: Theory and Application*, Prentice Hall, Upper Saddle River, NJ, USA, 1999.

[14] S. Haykin, *Adaptive Filter Theory*, 4th Edition, Prentice Hall, Upper Saddle River, NJ, USA, 2002.

[15] K. E. Baddour and N. C. Beaulieu, "Autoregressive models for fading channel simulation," in *Proceedings of IEEE Global Telecommunication Conference*, vol. 2, pp. 1187–1192, 2001 .

[16] C. K. Sung and I. B. Collings, "Spectrum sensing technique for cognitive radio systems with selection diversity," in *Proceedings of the IEEE International Conference on Communications*, pp. 1-5, May 2010.

[17] C. Komninakis, C. Fragouli, A. H. Sayed, and R. D. Wesel, "Multi-input multi-output fading channel tracking and equalization using Kalman estimation," *IEEE Transactions on Signal Processing*, vol. 50, no.5, pp. 1065-1076, May 2002.

[18] A. Ghasemi and E. S. Sousa, "Opportunistic spectrum access in fading channels through collaborative sensing," *Journal of Communications*, vol. 2, no. 2, pp. 71-82, March 2007.

[19] I. Glaropoulos and V. Fodor, "On the efficiency of distributed spectrum sensing Ad-hoc cognitive radio networks," *Proceedings of the 2009 ACM workshop on Cognitive radio networks*, pp. 7-12, September 2009.

[20] Z. Khan, J. Lehtomäki, K. Umebayashi, and J. Vartiainen, "On the selection of the best detection performance sensors for cognitive radio networks," *IEEE Signal Processing Letters*, vol. 17, no. 4, pp. 359-362, April 2010.

[21] A. Ghasemi and E. S. Sousa, "Collaborative spectrum sensing for opportunistic access in fading environments," *First IEEE International Symposium on New Frontiers in Dynamic Spectrum Access Networks*, pp.131-136, November 2005.

[22] V. I. Kostylev, "Energy detection of a signal with random amplitude," *IEEE International Conference on Communications*, vol. 3, pp. 1606-1610, August 2002.

[23] M. F. Pop and N. C. Beaulieu, "Limitations of sum-of-sinusoids fading channel simulators," *IEEE Transactions on communications*, vol. 49, pp. 699-708, April 2001.

[24] D. J. Young and N. C. Beaulieu, "The generation of correlated Rayleigh random variates by inverse Fourier transform," *IEEE Transactions on communications*, vol. 48, pp. 1114-1127, July 2000.

[25] N. M. Neihart, S. Roy, and D. J. Allstot, "A parallel, multi-resolution sensing technique for multiple antenna cognitive radios," *IEEE International Symposium on Circuits and Systems*, pp. 2530-2533, May 2007.

[26] A. Sonnenschein and P. M. Fishman, "Radiometric detection of spread spectrum signals in noise," *IEEE Transactions on Aerospace Electronic Systems*, vol. 28, no, 33, pp. 654-660, July 1992.

[27] W. A. Gardner, "Signal interception: a unifying theoretical framework for feature detection," *IEEE Transactions on Communications*, vol. 36, no. 8, pp. 897-906, August 1988.